JPL PUBLICATION 85-71

A Comparison of 8.415-, 32.0-, and 565646-GHz Deep Space Telemetry Links

R.M. Dickinson

October 15, 1985

National Aeronautics and
Space Administration

Jet Propulsion Laboratory
California Institute of Technology
Pasadena, California

JPL PUBLICATION 85-71

A Comparison of 8.415-, 32.0-, and 565646-GHz Deep Space Telemetry Links

R.M. Dickinson

October 15, 1985

National Aeronautics and
Space Administration

Jet Propulsion Laboratory
California Institute of Technology
Pasadena, California

The research described in this publication was carried out by the Jet Propulsion Laboratory, California Institute of Technology, under a contract with the National Aeronautics and Space Administration.

ACKNOWLEDGMENT

The author gratefully acknowledges the Ka-band task team members' material assistance.

Name	Discipline
Jim Boreham	Spacecraft Microwave
Al Bhanji and Rob Hartop	DSN Microwave
Jim Lesh and Jon Schwartz	Optical Communication
Bob Freeland	Spacecraft Structure
Verl Lobb and Sal Rocci	DSN Structure
Sam Sirlin	Spacecraft Attitude Control
Carl Gilchriest and Murray Koerner	Telecom System
Rod Zieger and Herb Phillips	Spacecraft Systems

ABSTRACT

An economic and performance comparison is made of spacecraft telecommunication links at 8.415, 32.0, and 565646 GHz (0.53-micron wavelength) for the return of 3.43×10^{11} bits from a Saturn Orbiter/Titan Probe mission in the year 2000.

Technical performance and costs for both ends of the links are included. Spacecraft antenna or telescope efficiencies, pointing losses, ground-based or Earth-orbiting relay terminals efficiencies, noise temperatures, recurring and nonrecurring engineering, and maintenance and operations costs are modeled. Weather effects, dc-to-RF or laser power conversion efficiencies, gravity and other environment distortions gain reductions, and the cost of pointing and tracking are analyzed in the study.

The effort was focused primarily on the microwave frequency links and, although originally intended to also cover the Mars Sample Return Rover Mission, little emphasis was given to it in the press for time.

There are large uncertainties in the cost results, but conclusions indicate that for a mid-1990's launch, the Ka-band system is as cost effective as X-band. When amortized over about four missions, the combined spacecraft and ground costs are approximately equivalent to what the X-band would cost. The Ka-band system has a data rate advantage as compared to the X-band system for the same dc power input to the spacecraft. The magnitude of the advantage is a complex function of the weather at the DSN stations and the elevation angle of the ground antenna. A simple numerical comparison of the advantage is difficult and therefore curves are provided.

The optical frequency link is more costly based upon the launch-to-orbit costs for the orbiting terminal. A more detailed study of the optical system is recommended to quantify astrometric tracking benefits and to improve the accuracy of the cost estimate.

Expenditures of nonrecurring engineering to make the transition to Ka-band are required, most particularly to improve by a factor of four both the spacecraft and ground antenna pointing and tracking capabilities as compared to X-band. An electronically steered transmitting array on the spacecraft and a phased array feed and possibly controllable surface panels are recommended for the DSN antennas, along with other improvements.

CONTENTS

Figures

Tables

SECTION I

INTRODUCTION

A 10-week study was commissioned in January 1985 to understand the relative value of X-band, Ka-band, and optical wavelength telecommunications systems for the return of deep-space exploration data. The cost and performance, as measured by the achievable downlink telemetry data rates resulting from improvements to the existing ground-based and space segment capabilities at 8.415 GHz (X-band), were compared to similar measurements for proposed 32.0-GHz (Ka-band) and 0.53-micron wavelength (optical frequency 565646 GHz) links.

A previous cursory comparison of optimized total flight and ground telecommunications related costs, based upon only recurring engineering costs assembled by the author [Ref. 1] had resulted in a conclusion that Ka-band had no advantage in cost over X-band, and that optical communication costs were the lowest of the three options. The assumptions were questionable (lacking traceability) and the nonrecurring engineering costs were not included. Therefore, a more in-depth study was commissioned.

A part of the motivation for the studies was the fact that combined with the requirement to produce low-cost missions [Ref. 2], the recent threat of an escalation in the cost of RTG power for deep-space exploration spacecraft has resulted in telemetry link designs at 8.415 GHz with reduced RF output power (less than 10 W, compared to more than 20 W previously). Consequently, there would be a low data-rate capability [Ref. 3]. The trade study would also assess the effects of this approach on the overall cost to NASA for data return.

The rationale for studying higher frequency systems is that the shorter wavelengths permit higher antenna gains on the spacecraft and the ground for the same physical aperture size. The theoretical net link advantage in data rate for fixed aperture antennas in space, with all other aspects being equal, is the square of the frequency ratio.

Nevertheless, higher frequencies suffer increased attenuation when propagating through the Earth's atmosphere and the atmosphere's emission contributes substantially to the noise temperature of the receiving system, which further degrades reception. Also, the environmental effects, manufacturing tolerances, required increased pointing accuracy, and lower dc-to-RF conversion efficiencies of RF power amplifiers all suggest a trade study to determine the net achievable advantages, in both performance and cost.

For example, as the cost of spacecraft dc power increases, there is a tendency to increase the spacecraft antenna gain to offset the effects of reduced RF output power. However, the spacecraft is affected by increased mass, power, and equipment for pointing the higher gain (narrower beamwidth) antenna. Detailed multisubsystem trade studies are required to determine the best course of action with the new constraints. Also, the interactions with and the effects on the ground terminal need to be analyzed, in particular, the effects of increased network loading resulting from lower data-rate spacecraft missions.

Previous studies comparing various microwave, infrared, and optical frequency links [Ref. 4] had determined that microwave links were best. However, the results were qualitative and are sensitive to a host of factors such as weather-related propagation statistical data, antenna performance, spacecraft dc-to-RF or optical conversion efficiency, antenna- or telescope-pointing accuracy and power requirements, and other factors whose performance and uncertainty magnitudes have changed in the interim. The advent of a permanent presence in space (Space Station) in the future is an example.

The microwave systems assume that the receiving terminal will be the 70-m antennas in the Deep Space Network (DSN). At both 8.4 and 32 GHz, the telemetry return costs to NASA were calculated for the performance of the current 64-to-70-m upgrade, as well as for potential improvements to the 70-m antennas to reduce gravity and other environment degradations to performance.

The optical system assumes a Space Station based photon bucket (non-diffraction limited optical collector), with subsequent relay of the telemetry to JPL via microwave links through the tracking and data relay satellite (TDRS) or tracking and data acquisiton system (TDAS).

An attempt was made to provide a fair comparison of the three different frequency systems. The method minimized the overall cost to NASA for the combined spacecraft and ground portions of the telemetry system for the same number of bits sent by each system.

The cost minimization process begins with determining the optimum minimum cost combinations of transmitter power and antenna gain aboard the spacecraft for any given gain-power product (or effective isotropic radiated power, eirp). Then, for a given total number of bits of data to be returned and for a given DSN data-rate support capability, the eirp is determined at each frequency that results in the minimum combined spacecraft and ground costs.

The conclusions of the study are that Ka-band has a definite performance advantage over X-band. For a 0.90 reliability link at Goldstone the advantage is 6.8 dB at a 50° elevation angle and 2.4 dB at 10°. At Canberra or Madrid, the corresponding advantages are 6.2 and 0.5 dB, due to a weather model difference from Goldstone.

The difference in cost between X-band and Ka-band is small and much less than the uncertainty in the cost estimates.

There are viable approaches to the increased pointing accuracy at 32 GHz required on both spacecraft and ground antennas. Examples are an electronic-beam steered array on the spacecraft and an active multi-element receiving array and/or mechanically positioned surface panels on the ground antenna.

The optical system costs are larger and more uncertain than the microwave system costs due to technical maturity and the cost of transporting, assembling, and operating a spaceborne optical-microwave relay terminal.

In addition to cost constraints, the spacecraft design is determined by the requirements of the missions which are discussed in the next section.

SECTION II

MISSION SET AND METHODOLOGY

A. MISSION SET

In order to perform a realistic trade study to properly assess the higher frequency links, requirements for the telemetry systems were determined from two classes of deep-space mission sets selected as candidates from among the recommended missions of the Solar System Exploration Committee (SSEC) of the NASA Advisory Council. The Saturn Orbiter/Titan Probe (SOTP) and the Mars Sample Return (MSR) Rover were felt to be representative of most of the missions in Table 1.

The SOTP mission has, as its principal requirement, the return of 3.43×10^{11} bits (from 11 AU maximum range) during its two-year orbiting tour around Saturn and its moons (Table 2). The quantity of information returned via the telemetry link was determined from the end-to-end information system study [Ref. 5] by summing the products of the DSN tracking times and the corresponding downlink rates required during the various mission phases. The downlink data includes images that are compressed (4:1) aboard the spacecraft before being assembled in packets with other science and engineering telemetry, Reed-Solomon coded, and convolutionally encoded for transmission.

The MSR Rover plans to return 6.7×10^{10} bits from Mars (maximum range 2.683 AU) during its Martian year (687 Earth days) traverse goal of 100 km [Ref. 6].

B. METHODOLOGY

One objective of this trade study was to determine which frequency downlink telemetry system is most cost effective to satisfy the data-return requirement. In the past, a typical design approach was to simply determine the data rate that each different frequency's affordable technology would support, and to declare that the highest data-rate system was best. That was before the escalation of the cost of spacecraft power)(a change in the method of allocation of RTG costs among Federal Agencies (private communication from R. Draper, Dec. 1984), which resulted in the approach of designing for a minimum data rate in order to reduce the spacecraft cost.

However, a minimal performance spacecraft that reduces the flight project costs affects the other arm of NASA, tying up the DSN for long periods of time to return the mission data at such a low rate. This loading of the Network could result in NASA having to construct or rent additional ground antenna aperture in order to adequately serve its other customers. A better design approach may be to ask what data rate during the data return periods will result in the least overall cost to NASA, then to let that result determine the spacecraft design data rate.

Table 1. Solar System Exploration Mission Set

	MISSION	PROJ. START	SYSTEM TEST	LAUNCH	DEEP SPACE Δ	GRAVITY ASSIST	ENCOUNTER	NEOM*	COMMENTS
PLANETARY OBSERVERS	MGCO	FY'85	89/90	8/90	–	–	8/91	8/93	BEGIN MAP ORBIT: 10/91
	LGO	FY'88	90/91	12/92	–	–	12/92	12/93	115^h TRANSFER
	NEAR EARTH ASTEROID RENDEZVOUS	FY'89	92/93	6/94	–	–	6/95	6/96	ASTEROID ANTEROS
	COMET INTERCEPT SAMPLE RETURN (KOPFF)	FY'91	87/88	12/94	–	–	7/96	12/96	
	MARS AERONOMY ORBITER	FY'91	99/95	10/96	–	–	11/97	11/98	
	MARS SURFACE PROBE	FY'93	96/97	10/99	–	–	10/00	10/01	SIX SURFACE
MMII'S	COMET RENDEZVOUS/ ASTEROID FLYBY (WILD 2)	FY'87	90/91	3/91	–	–	1/95	10/97	4+ AU INBOUND, T_p: 5/7/97
	SATURN ORBITER *WITH TITAN PROBE*	FY'90	92/93	5/94	12/95	7/97(EARTH)	10/01	10/01	
	URANUS FLYBY URANUS PROBE	FY'96	95/96	2/97	–	(JUPITER)	12/03	4/04	
	MAIN BELT ASTEROID RENDEZVOUS #1	FY'96	98/99	2/00	–	–	1/02	9/06	
	SATURN FLYBY WITH SATURN PROBE	FY'99	01/02	7/03	–	(JUPITER)	3/06	7/06	
AUGMENTED	MARS SAMPLE RETURN	FY'92		11/96				9/99	
	COMET NUCLEUS SAMPLE RETURN	FY'93		/97				/03	

*NEOM = Nominal End of Mission

Table 2. SOTP Mission Data

Events	Dates	Mission Tracking Time and Data Rate	Subtotal #Bits	Mission, %
Project Start	90			
Technology Cutoff	91			
System Test	92/93			
Launch	5/94			
Deep Space ΔV	12/95			
Gravity Assist (Earth)	7/97			
Cruise		8^h/week for 6 yrs @ 1.2 kbps	= 1.078×10^{10}	3.1%
Far Encounter		8^h/day for 60 days @ 9.3 kbps	= 1.607×10^{10}	4.7%
Saturn Encounter	10/01	24^h/day for 48 days @ 6.1 kbps	= 2.53×10^{10}	7.4%
Post Encounter Playback		24^h/day for 43 days @ 7.2 kbps	= 2.675×10^{10}	7.7%
Orbit Cruise		8^h/day for 850 days @ 10.8 kbps	= 26.438×10^{10}	77.0%
NEOM	12/03			
			Σ = 34.328×10^{10} bits	100%

The total cost will be derived from the costs for power and mass transport of the spacecraft and the ground costs. A pictorial of the data-return system cost model showing the spacecraft telecommunications-related elements and the separate ground-based cost elements is shown in Figure 1.

C. SPACE SEGMENT ELEMENTS

The spacecraft eirp is determined by the transmitter output power and the antenna gain. The cost is sensitive to how the gain-power product is apportioned between the two. If the transmitter power is selected too low, then the antenna cost will be too high to achieve the desired product. Conversely, too large a transmitter and too small an antenna will also cost more than is necessary. The optimum or minimum cost determination is complex, due to such factors as the transmitter dc-to-RF conversion efficiency, which is a function not only of frequency, but also of the output power level. Curves of the dc-to-RF power conversion efficiencies of X-band and Ka-band spacecraft power amplifiers developed by Jim Boreham are shown in Figures 2 and 3. The efficiencies of the required dc-to-dc power converters (or high-voltage power supplies) are included, along with the losses in transmission lines, as required to deliver the amplified transponder output to the antenna input connector.

The transmitter, in addition to requiring spacecraft dc power, also has mass to be transported, consisting of its own and supporting equipment mass such as the baseplate required for thermal waste heat removal. Additionally, the portion of the spacecraft power that is required by the transmitter must be assessed its proportionate share of the mass of the RTG power unit.

The antenna has mass that must be transported and, although one normally thinks of it as a passive structural element, its prime function requires dc power and additional equipment and propulsion mass that must be utilized to point the antenna, otherwise the antenna gain will not be realized.

Figure 4 shows the magnitude of the pointing problem in the form of gain loss in dB as a function of peak pointing error for selected diameter antennas in the frequencies of interest. The current Galileo pointing-system, baseline specification is also shown, along with indicated points for improved sensor knowledge and reduced deadbands. Sample electronic beam steered (EBS) (phased array) pointing losses are also indicated for array feeds instead of the current focal point or cassegrain single-point feeds. Table 3 (private communication from J. Boreman and S. Sirlin) shows the pointing control options considered in this study.

Some fraction of the cost, mass, and dc power of the attitude control system reference units, the pointing control system computer operations, and the various actuators must be included in a fair accounting. However, as the attitude control system provides services for other subsystems and functions such as instrument pointing and trajectory changes, only a fraction of its mass and power was charged to antenna telemetry return pointing. In this study, a rather arbitrary 20% of the spacecraft attitude control system was ascribed to telecom pointing.

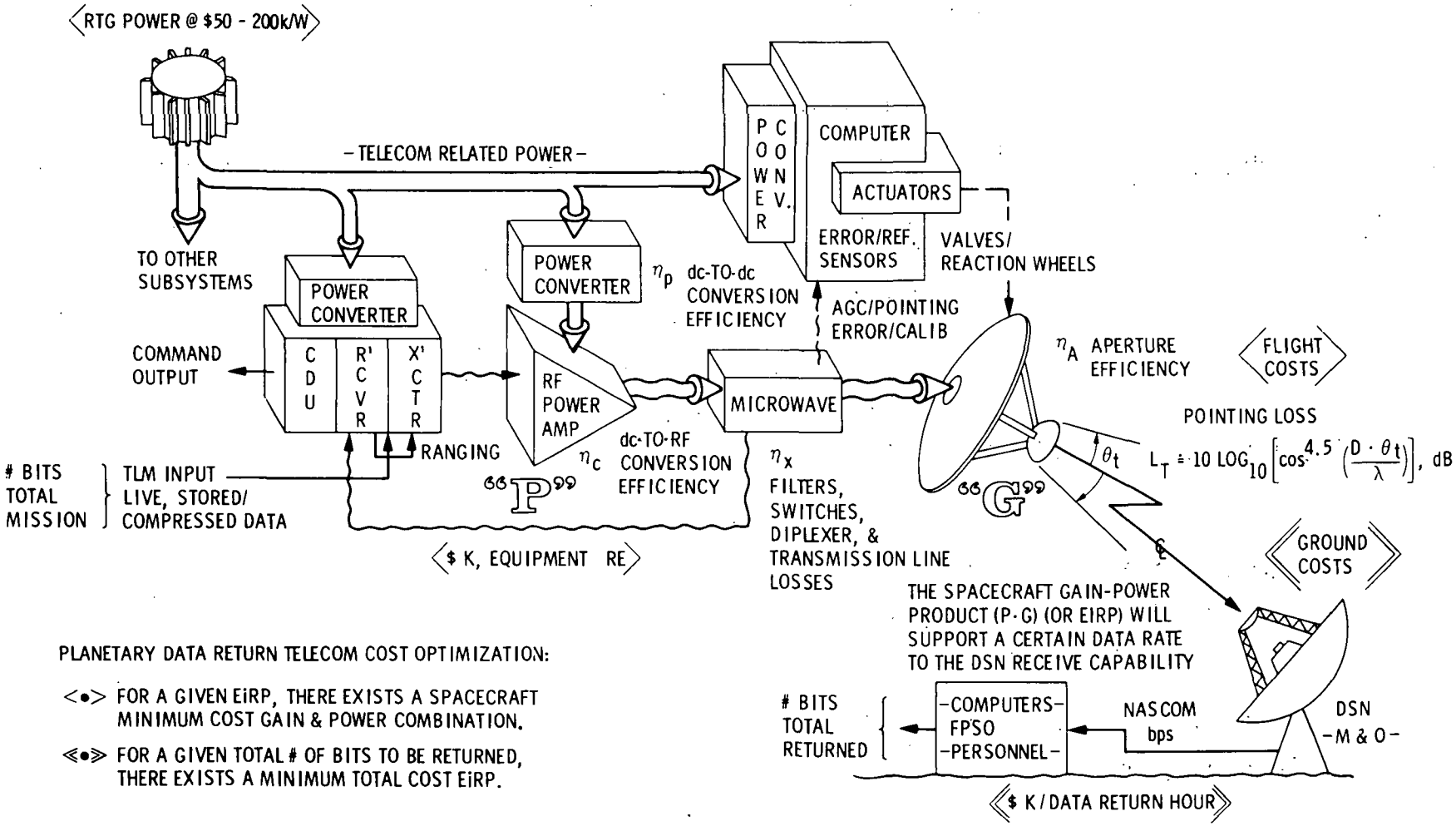

PLANETARY DATA RETURN TELECOM COST OPTIMIZATION:

<•> FOR A GIVEN EIRP, THERE EXISTS A SPACECRAFT MINIMUM COST GAIN & POWER COMBINATION.

≪•≫ FOR A GIVEN TOTAL # OF BITS TO BE RETURNED, THERE EXISTS A MINIMUM TOTAL COST EIRP.

Figure 1. Deep-Space Planetary Exploration Data Return System Cost Model

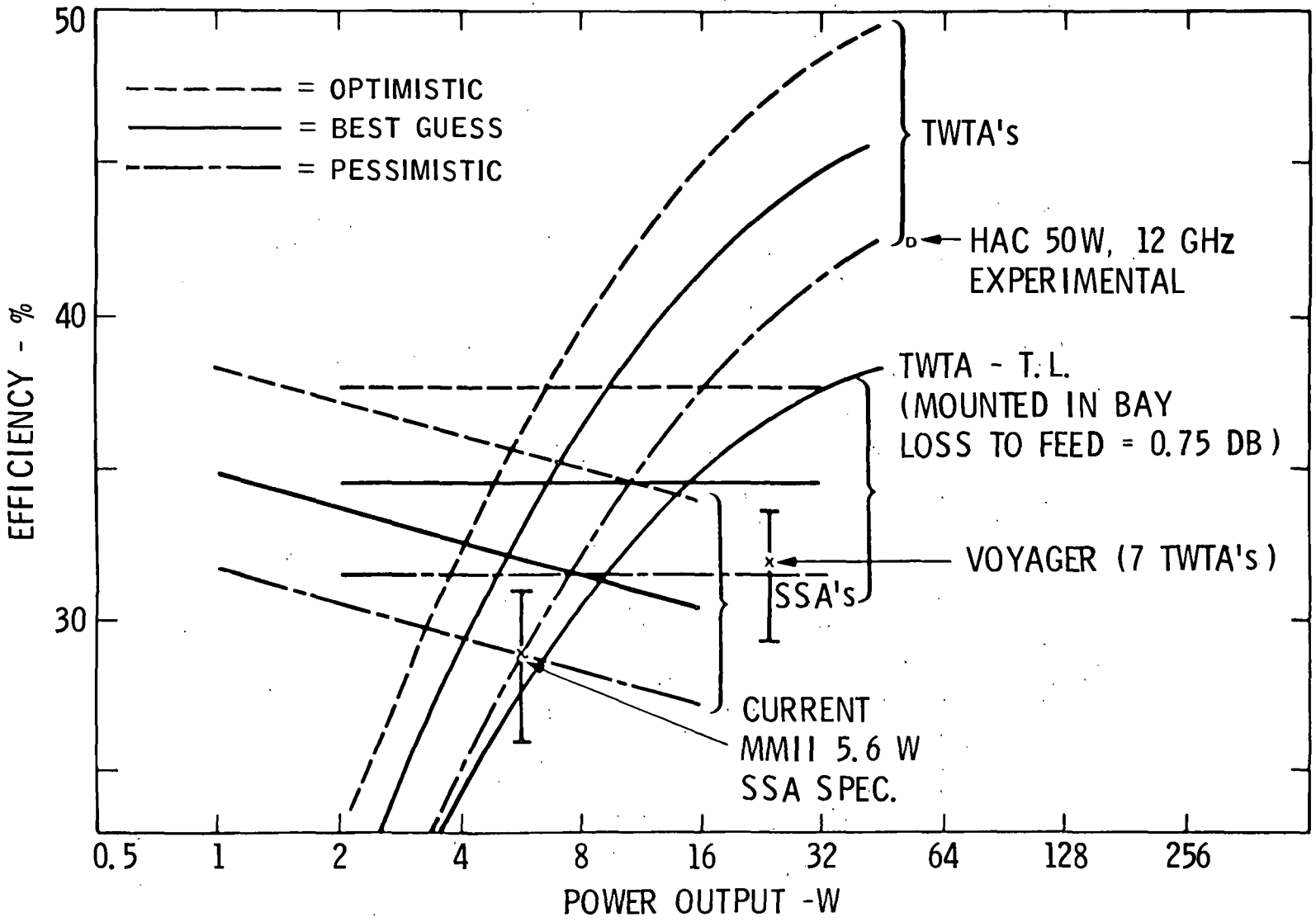

Figure 2. Spacecraft X-Band Power Amplifier Efficiencies

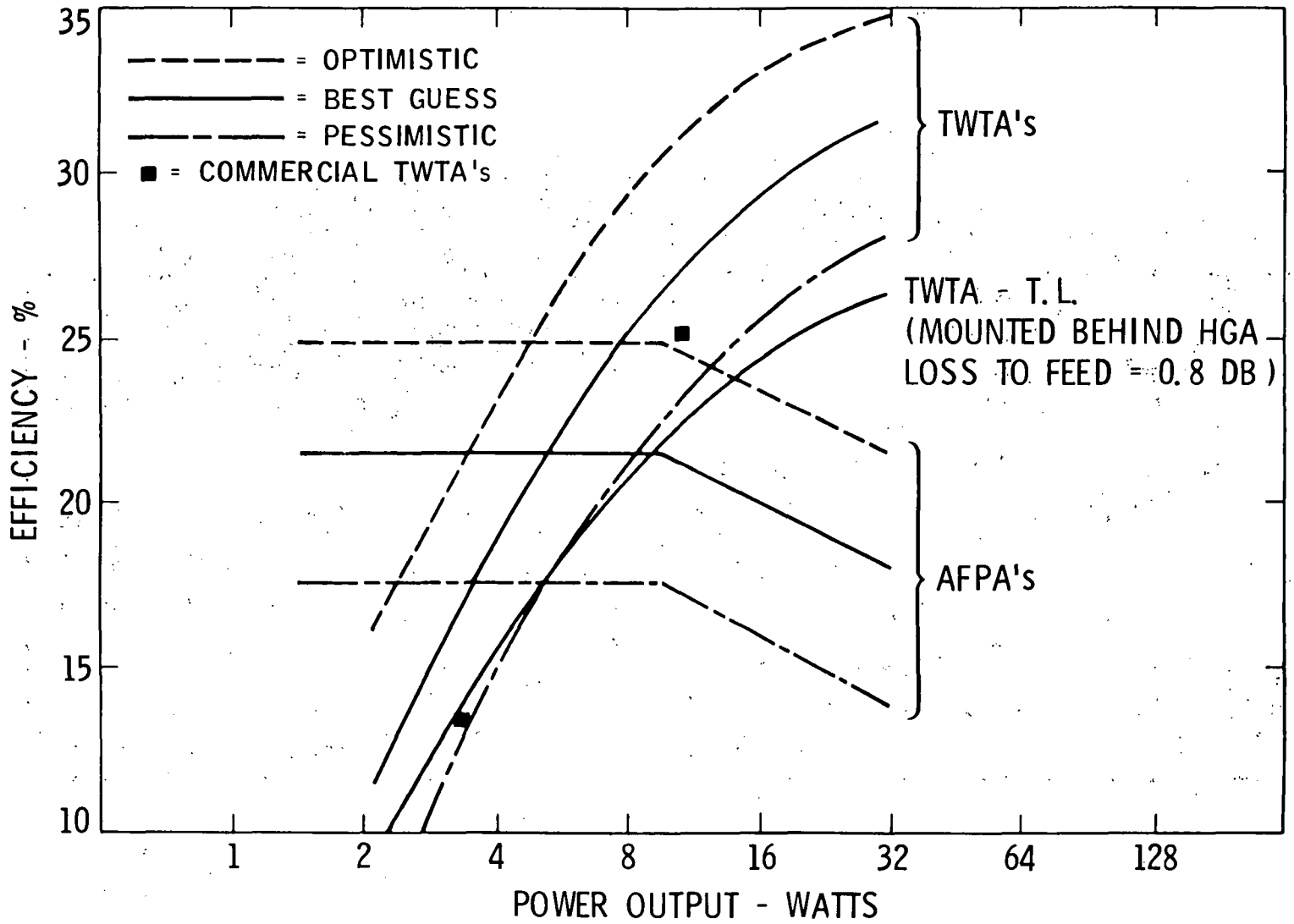

Figure 3. Spacecraft Ka-Band Power Amplifier Efficiencies

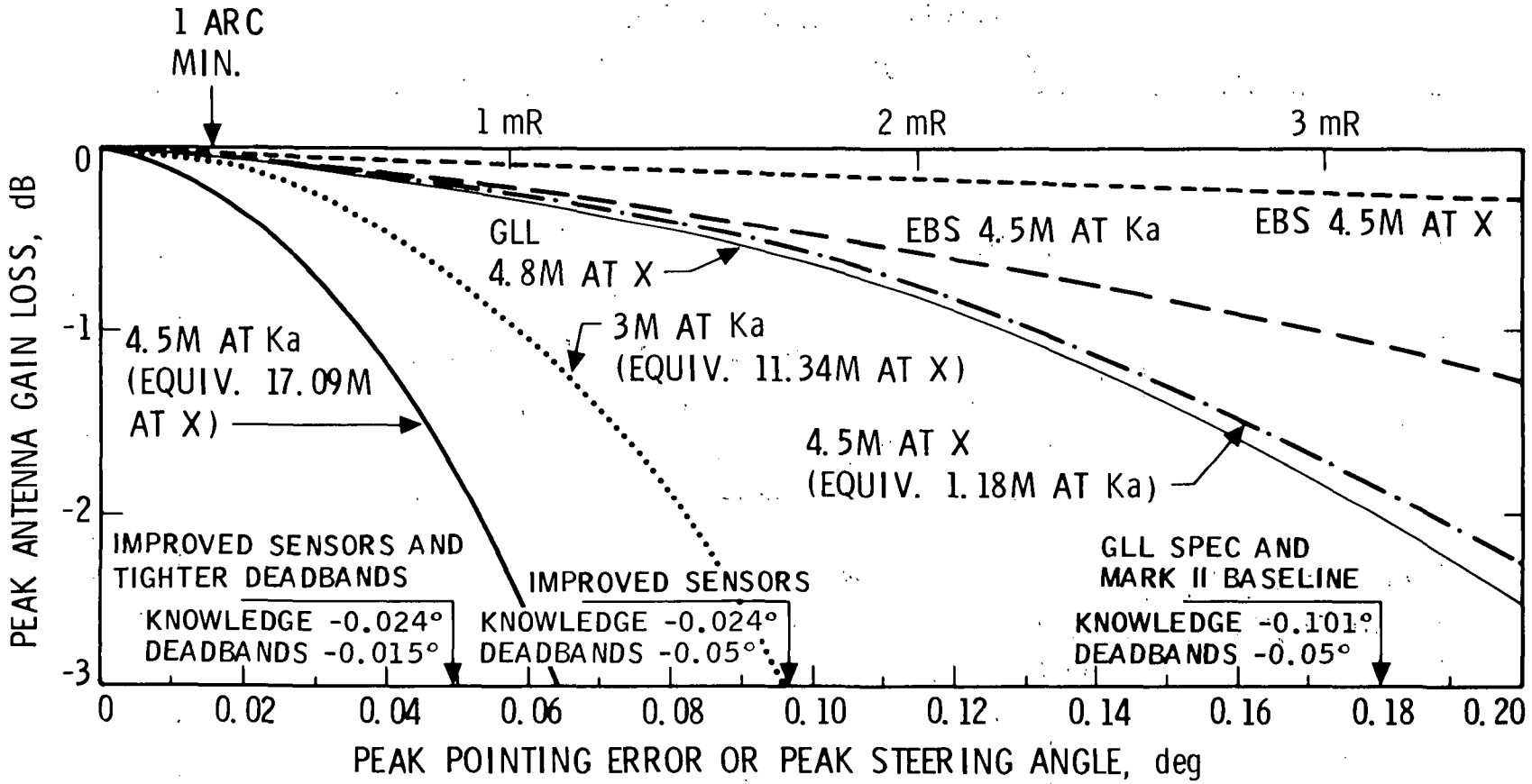

Figure 4. Achieving Spacecraft Antenna Gain

Table 3. Ka-Band Spacecraft Pointing Control Options

CONTROL ACTUATORS	SENSORS	DEADBAND PER AXIS	SENSOR/ ALIGNMENT ERRORS* 2 AXIS	TOTAL 2 AXIS ERROR	MASS kg	PWR W	1st USER COST M$***	2nd USER
0.2N THRUSTERS	MMII BASELINE	0.05^0	0.094^0	0.165^0	17	15	7.1	7.1
0.2N THRUSTERS	UPGRADED	0.05^0	0.025^0	0.097^0	10	10	9.4	4.8
PULSE PLASMA** THRUSTERS	UPGRADED	0.015^0	0.025^0	0.046^0	71	15	17.6	
REACTION** WHEELS	UPGRADED	0.0055^0	0.021^0	0.025^0	14	40	17.7	12.6
EBS**	UPGRADED	0.05^0	0.025^0	0.030^0	14	12	15.6	8.3
EBS**	MONOPULSE	0.05^0	0.005^0	0.011^0	15	14	17.9	9.3

*ITEMS INCLUDE - STAR TRACKER, GYRO, PLATFORM POSITION TRANSDUCER, STRUCTURAL ALIGNMENT, VARIATION IN DEADBAND (17.1%)

**REQUIRES 0.2N THRUSTERS AND UPGRADED SENSORS

***INCLUDES RE, NRE, AND COST OF MASS AND POWER AT $80 K/kg AND $200 K/W FOR ALL EQUIPMENT REQUIRED

(Typically, if the antenna pointing requires mass expulsion, then additional cost for mass transportation must be attributed to the antenna in proportion to the fraction of that resource devoted to keeping the beam directed to Earth for communication purposes. A cost allocation of the portion of the attitude control and propulsion subsystems to the antenna subsystem should probably be based upon the percentage of the time of the mission that is devoted to telecommunication high-gain antenna pointing, weighted by the precision required for that portion of the mission. If the spacecraft attitude control is simultaneously occupied with performing high-gain antenna and instrument pointing at the same time, for example, then the cost apportionment should be split based upon the relative precision required by each. These parenthetical considerations were not incorporated in the study results.)

A further portion of a spacecraft subsystem cost that must be attributed fairly to the various frequency telemetry systems being studied, is the applicable fraction of the cost of data storage. This is because of the potential unavailability of the DSN due to weather outages, scheduled or unscheduled maintenance, or the Earth occultation of a low earth-orbiting (LEO) space station or platform on which the optical frequency photon bucket resides. Again, less than 100% of the data storage mass and power cost is attributable to this condition, as the spacecraft requires data storage when it is occulted by a planet or a moon, due to trajectory design. Of the cost of data storage, 66% was attributed (equally and thus incorrectly) to each of the three options.

Figure 5 shows the costs for tape recorder data storage and playback aboard the spacecraft. In general, it would be expected that the higher frequency links would be more subject to DSN unavailability because of the greater severity of weather effects.

Similarly, the data compression mass and power costs are to be considered in the trade study due to the marginal cost of compressing data compared to the cost of increasing the spacecraft eirp or the ground gain-to-noise temperature ratio. There are associated costs for ground-based (data recompression), as well as spaceborne equipment to be considered. This study arbitrarily picked 88% of the data compression equipment cost, mass, and power to be applicable to the performance of the telecom function.

Other spacecraft subsystems costs, such as science instruments, were not considered as they were common to the three frequencies.

D. GROUND SEGMENT ELEMENTS

At the Earth end of the telemetry links, the atmosphere and weather effects were taken into consideration in comparing the microwave links. Weather affects the performance of the receiving system by attenuating the downcoming signal and raising the effective noise temperature of the receiver, thus decreasing its sensitivity. Wind loading and antenna surface or structure temperature differences distort the reflector surface and change the gain and beam pointing. The weather effects are site specific, in that Goldstone at its geographical location and higher elevation has on the average a drier climate than either Madrid or Canberra. Table 4 [Ref. 7] shows the

	NIMBUS	MM'71	LM-DESCA	WBVTR	VIKING	VGR	GLL	MMK II	VRM
DESIGN AND DEV.	1.034	5.000	3.986	5.629	8.179				
HDW	0.230	0.498	0.106	1.090	0.596				
1979 $ TOTAL	1.264	5.498	4.092	6.719	8.775		81 3.5	1.5*	3.0
INFLATION	1.36	→					1.24	-0-	1.06
1985 $ M	1.72	7.48	5.56	9.14	11.93		4.34	1.5	3.18
STORAGE BITS	9.79×10^{7}	1.8×10^{8}	3.6×10^{6}	3.0×10^{10}	6.72×10^{8}	5.5×10^{8}	9.0×10^{8}	9.0×10^{8}	1.8×10^{9}

*RESIDUAL HDW

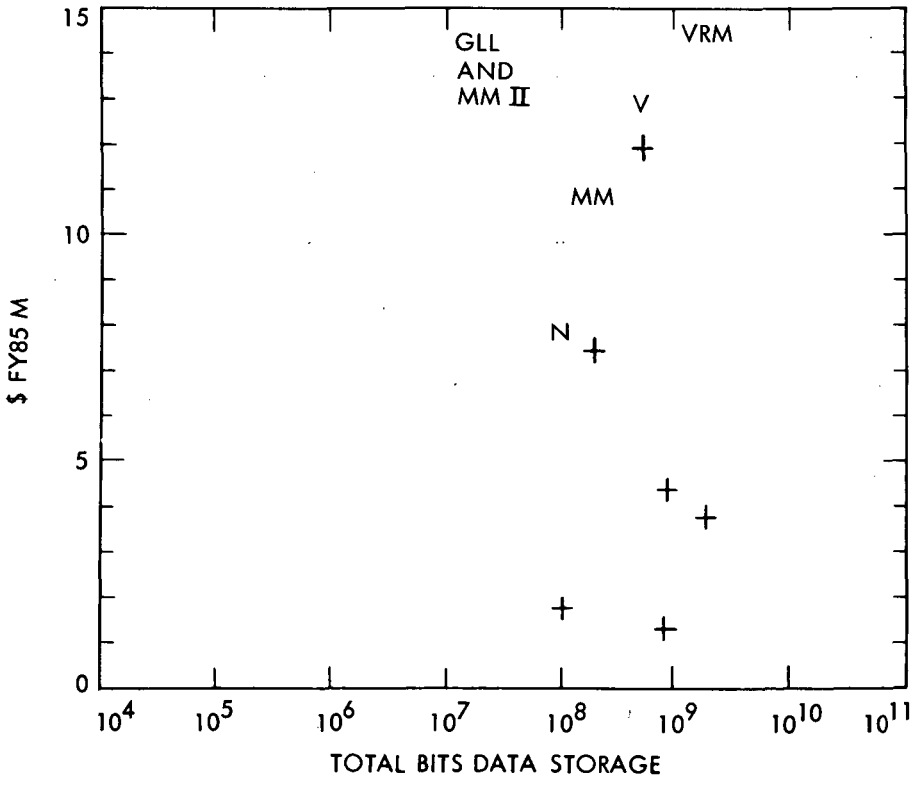

Figure 5. Spacecraft Tape Recorder Costs

Table 4. Thirty-Degree Elevation Angle: a) Ka- and X-Band Atmospheric Models for Goldstone; and b) 1985-era DSN Receiving System Noise Temperatures

a)

1. Cumulative distribution (% time)	0	50	80	90	95	98	99	99.5
2. Ka-band noise temperature model, K	9.84	19	25	29	35	43	53	69
3. Ka-band water vapor, cloud, rain contribution, K	0	9.16	15.16	19.16	25.16	33.16	43.16	59.16
4. Water vapor, clouds, rain, modelled to X-band, K	0	0.65	1.07	1.35	1.77	2.34	3.04	4.17
5. X-band total noise temperature, K	3.54	4.19	4.61	4.89	5.31	5.88	6.58	7.71
6. Ka-band attenuation, dB	0.15	0.29	0.39	0.45	0.54	0.67	0.82	1.07
7. X-band attenuation, dB	0.05	0.06	0.07	0.076	0.082	0.09	0.10	0.12
8. Ka-band system noise temperature, K	25.84	35	41	45	51	59	69	85
9. X-band system noise temperature, K	21.54	22.19	22.61	22.89	23.31	23.88	24.58	25.71
10. Ka-band attenuation above baseline, dB	0	0.14	0.24	0.30	0.39	0.51	0.67	0.92
11. X-band attenuation above baseline, dB	0	0.01	0.02	0.026	0.032	0.04	0.05	0.07
12. Δ_{SNR}, Ka-band, dB	0	1.46	2.24	2.71	3.34	4.10	4.94	6.09
13. Δ_{SNR}, X-band, dB	0	0.14	0.23	0.29	0.37	0.49	0.62	0.84
14. Ka-band link SNR relative to X-band, dB	0.89	-2.21	-2.90	-3.31	-3.86	-4.51	-5.20	-6.14
15. Net Ka-band link SNR advantage relative to X-band (11.51 dB + line 14)	10.62	9.30	8.61	8.20	7.65	7.00	6.31	5.37

b)

Contributor	Ka-band	X-band
Maser and plumbing, K	7.3	8.9
Cosmic background, K	2.2	2.6
Ground radiation, K	6.5	6.5

cumulative probability effects of weather on the receiving system noise temperature, for 30° elevation.

Additionally, the atmosphere effects are elevation-angle dependent in that the receiver sees a greater quantity of water and oxygen molecules along the signal path at lower elevation angles. Figure 6 (private communication from S. Slobin, Feb. 1985) shows the Goldstone and Madrid or Canberra, average-year, relative system noise temperature at both X- and Ka-bands.

The ground antennas' pointing and tracking problems are illustrated in Figure 7. Along with the dB-pointing loss is shown the estimated cost for tracking-system development. The current 64-m antenna 810-5 pointing specification [Ref. 8], its reported performance, and the 70-m requirements at X- and Ka-bands are shown. A distinction should be made between pointing, which is done blind without feedback correction, and tracking, which requires feedback and pointing. The tracking acquisition range must lie within the pointing uncertainty boundaries.

The ground system operations costs considered were maintenance and operations of the network under consideration, the improvements proposed at X- or Ka-band, both NRE and RE at three DSN sites, the applicable cost to NASA of the NASCOM network for transporting the data from the DSN sites to JPL, and the proportionate cost of operating the NASCOM terminals at JPL, the fraction of the Flight Project Support Office (FPSO), and mission operations personnel and equipment associated with data return. Data processing and distribution costs will not be included as they are common to both frequencies.

NASA continues to support portions of the ground operations cost elements independent of usage demand. Nevertheless, for a loaded network, the available tracking time is a constrained resource. Therefore, a rate measure of value such as operations cost per unit of time must be attributed to DSN time in connection with a flight project's total cost to NASA. There are other customers requesting DSN service such as other existing or proposed flight projects within NASA, as well as foreign projects on a reimbursable basis, or other nations joint-tracking experiment support.

This demand in connection with the DSN service tradition creates a market. The service has value. Also, NASA has the option in slack times of mothballing selected subnets, or conversely, choosing to upgrade performance of existing plants or constructing or renting added apertures from other domestic or foreign sources in forecasted or actual times of peak or special loading. Some unit of value is required to permit the objective trade between flight and ground capability and can be used in connection with determining service priorities to various customers.

E. OPTICAL ELEMENTS

For the optical system, the transportation costs to LEO, and the Space Station astronaut EVA time for maintenance and operations were considered also. NASCOM costs were different in that TDRS was used to relay the data to Earth.

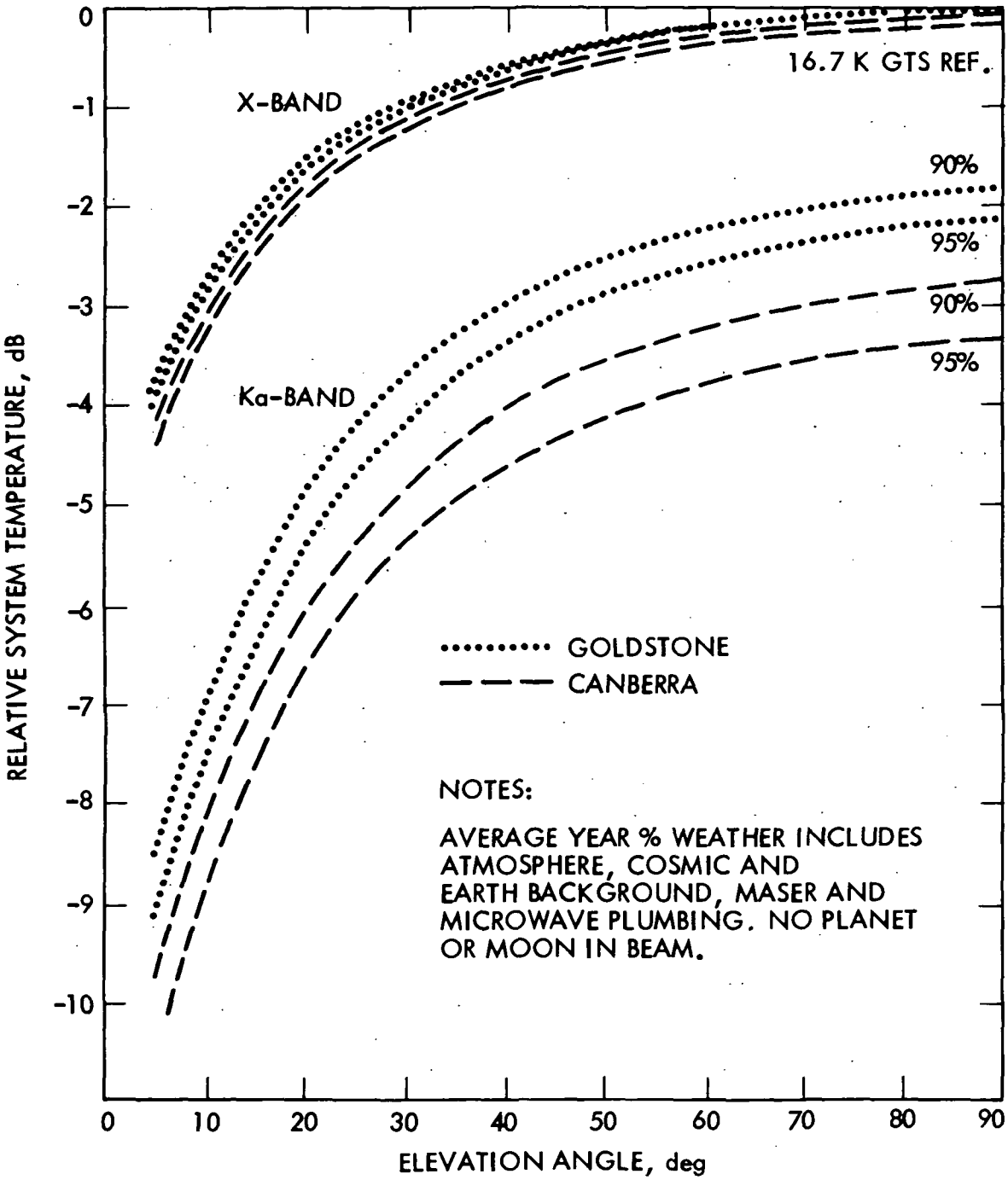

Figure 6. The 70-m Antenna Receiving System Noise Temperatures

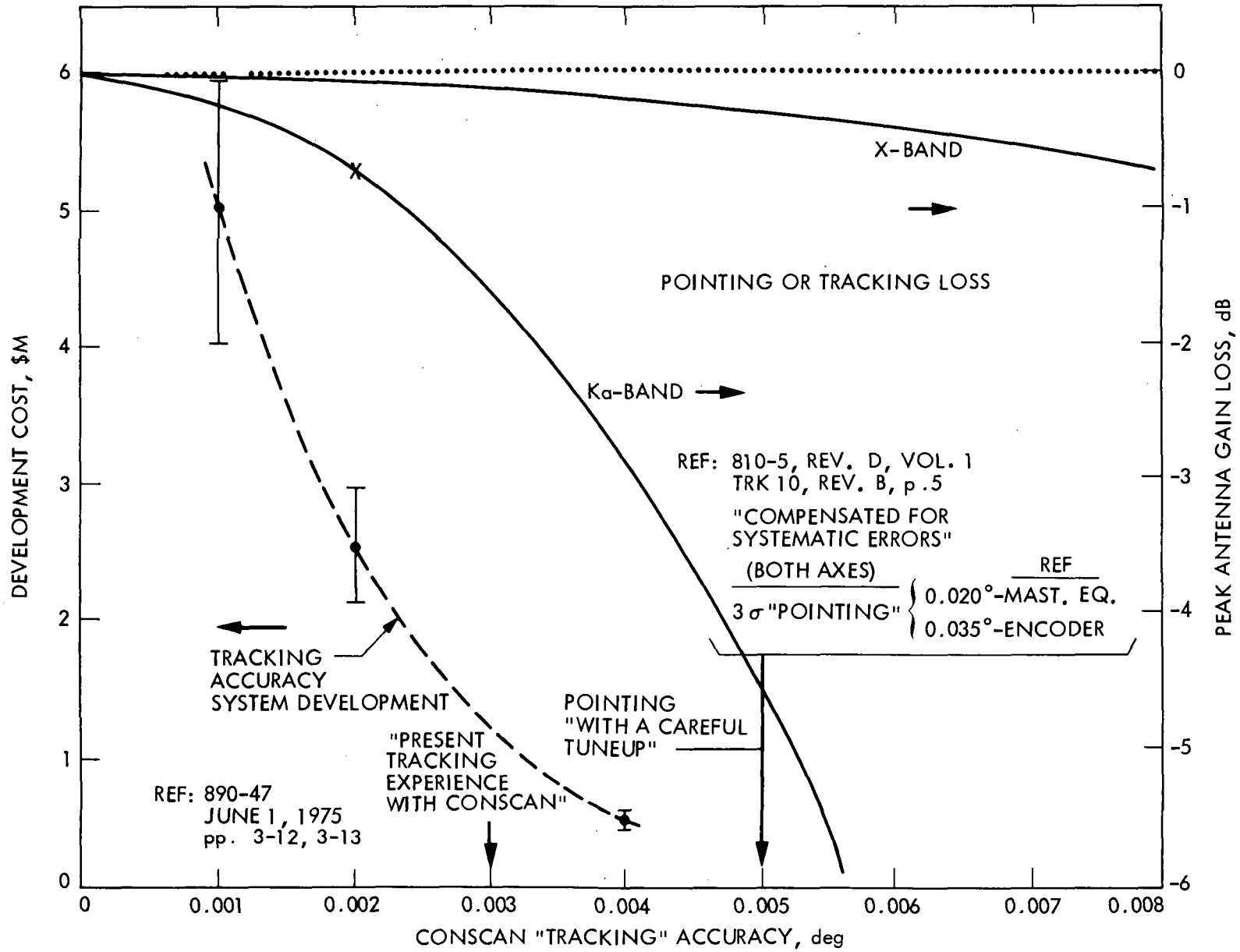

Figure 7. Achieving 70-m Ground Antenna Gain

A Supercalc 3 program on an IBM PC/XT was used to provide a means of collecting the various costs of the different frequency systems. The X-band system will be described first.

SECTION III

SYSTEM DESCRIPTIONS AND PARAMETER VALUES

Some elements and cost parameters of all three systems are common, and will be described first. Then the individual differences will be discussed.

A. GENERAL

All three systems have a common dc power cost on the spacecraft that was varied, to determine its sensitivity, from \$160K/W to \$240K/W, with \$200K/W as the design value (as compared to \$50K/W in the past) (private communication from R. Draper, Dec. 1984). The RTG power system specific mass was taken to be 2.1 W/kg optimistic, to 2.3 W/kg pessimistic, with a nominal 2.205 W/kg.

A nominal Shuttle launch cost to NASA is estimated at \$140M and a centaur G-prime upper stage cost at \$60M (private communication from R. Klemetson, Oct. 10, 1984). Thus, for injecting 2500 kg on an interplanetary trajectory, the transportation cost rate is pegged at \$80K/kg. The rate was varied from a \$36K/kg optimistic value to a pessimistic \$120K/kg.

The ground operations cost nominal rate was taken to be \$8500/hr, composed of a DSN 70-m network antenna reimbursable rate of \$2500/hr (private communication from J. Justice), a FPSO rate of \$3420/hr (based upon a Norm Haynes DRD viewgraph, Sept. 17, 1984, showing an average 250 headcount total MO and DA workforce for FY84 through FY89, and assuming \$120K/yr each for a 8760-hr year), and the remainder due to NASCOM and JPL mission support (the Mariner Mark II allocation of one million per month for cruise operations equals \$1389/hr). The optimistic and pessimistic rates were taken to be $\pm$20%, or \$6800/hr and \$10,200/hr, respectively. (For comparison, the total DSN FY85 budget, for a particular division, of \$65,328K yields an hourly rate of \$7457/hr.)

The spacecraft microwave-antenna, mass per unit area was 2.44 kg/m^2, $\pm$10%. The solid aperture-type antennas' cost was modeled as a constant recurring engineering cost of \$650K, $\pm$10%, plus a variable \$53K/m^2, $\pm$10%. The antenna costs and mass as a function of diameter and surface accuracy are shown in Figure 8 (private communication from R. Freeland).

All three frequency systems are to return 3.43 X 10^{11} total bits from 11 AU to JPL. Concatenated Reed-Solomon and convolutional coding are utilized to permit 4:1 average data compression with a channel bit error rate of 10^{-6} or less. The Earth-based microwave systems' performance was compared at a 30° elevation angle and for 90% weather model effects on receiving system noise temperature and atmospheric attenuation.

The effects of Earth weather on the microwave system performance differs with the two frequencies, due to the difference in wavelength of the radiation [Ref. 9]. More of the shorter wavelength electromagnetic energy is involved in energy exchanges with the molecules of the atmosphere and, consequently, there are more losses of energy and stimulations of incoherent radiation

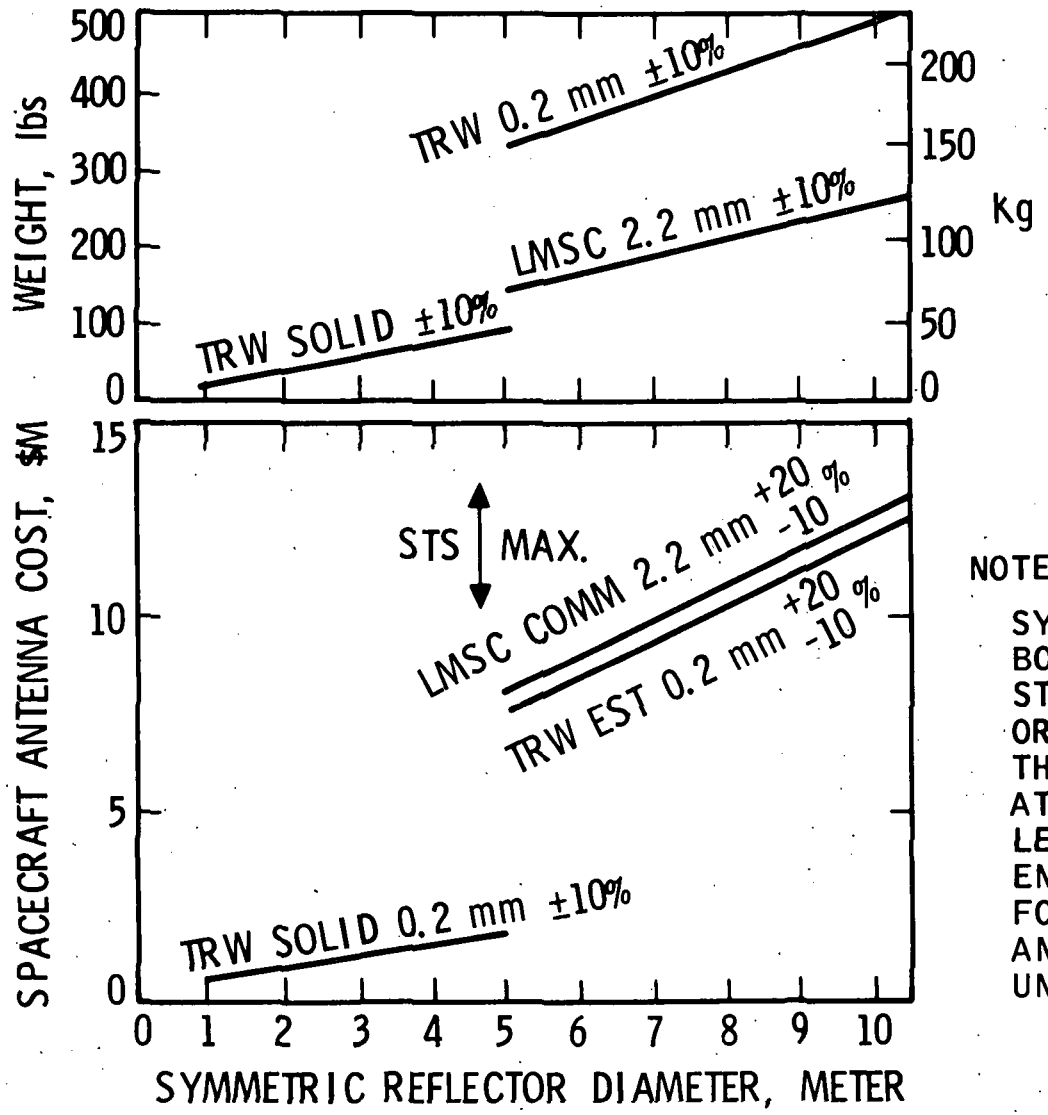

NOTES:

SYMMETRICAL REFLECTOR AND BOLTDOWN FLANGE AND SUPPORT STRUCTURE FOR FEED (NO FEED OR WAVEGUIDE INCLUDED). THERMAL AND MECHANICAL TESTS AT MECHANICAL SUBSYSTEM LEVEL (NO RF TESTS). ENGINEERING MODEL REFURBISHED FOR PROTOFLT. COST OF 2nd ANTENNA ~ 40-60% OF INITIAL UNIT.

Figure 8. Spacecraft Antenna Mass and Cost

leading to higher background noise. The skirts of a molecular oxygen absorption and radiation line at 60 GHz in conjunction with the water vapor lines at 22 GHz and higher frequencies contribute to these effects.

Propagation differences in performance at the different frequencies are caused not only by the uncondensed gases, but also by particles in the atmosphere such as dust, ash, pollen grains, insects, birds, and water in its condensed or frozen forms, which leads to additional losses by scattering and absorption. Thus, the atmosphere state in terms of the amount, type, and distribution of particles bears on the relative performance of the two microwave frequencies.

The attenuation due to precipitation-sized particles in our wavelength range of interest is inversely proportional to the square of the wavelength. Since weather (and not biological elements) is the predominant long-term propagation feature, we picked the 90% condition weather for our performance comparison. Only 10% of the time during an average year would we expect to encounter more severe weather at the specific DSN sites in question. [This selection may have been a bit optimistic as the Galileo Project uses telecom link design control tables with an overall link reliability of 95%, obtained by convolving the design element tolerance distributions with the weather probability (private communication from M. Koerner). A one-to-one correlation of link reliability and weather probability is not possible.]

B. DSN ANTENNAS

Table 5 lists the cost estimates for potential changes to the 70-m antenna to improve Ka-band performance. The study group selected the following subset.

The reference X-band 70-m antenna at the completion of the currently scheduled 64-to-70-m upgrade, is assumed to have its surface panels set at 45° elevation angle. A less than 20-mph wind is assumed to be blowing, thermal effects on the antenna structure are included, the surface panel rms manufacture error is less than $\pm$0.02 cm (0.008 in), the panels are set to $\pm$0.038 cm (0.015 in) accuracy, and conscan tracking to $\pm$0.002° is assumed. Table 6 (private communication from A. Bhanji) shows the resulting nominal efficiency factors, relative to a uniformly illuminated aperture. Also included are gain degradation factors due to aperture phase errors caused by atmospheric turbulence [Ref. 10].

The 70-m antenna performance as a function of elevation angle is shown in Figure 9 for the antenna gains, and Figure 10 for the combined gain-to-noise temperature ratio (G/T) performance that includes the sky noise temperature and sidelobe and backlobe noise contribution effects on the receiving system performance. Separate figures are shown for the Goldstone site and Madrid or Canberra, as Goldstone with its higher elevation and drier climate area has a decided advantage at the higher frequency.

The symmetrical gravity sag effect on the structure-related performance about 45°, as a function of elevation angle, is further modified by the effect of looking through additional atmosphere path length at the lower elevation

Table 5. Potential Improvements to 70-m Antenna to Increase Ka-Band Performance

	NRE	RE for 3 Sites	Sum and Tol. $K
1. New 0.0102 cm (0.004") rms Tol. Panels [vs. 0.0203 cm (0.008")]	500	9000	9500 ±20%
2. Precision Setting Panels			
0.0508 cm (0.025")	0	300	300 ±5%
0.0381 cm (0.015")	0	750	750 ±5%
0.0254 cm (0.010") holography	100	1050	1150 ±5%
0.0127 cm (0.005") required	350	1350	1700 ±20%
3. Reinforce Structure (0.0152 cm vs. 0.254 cm) (0.006" vs. 0.010") for wind and gravity sag	700	4950	5650 ±15%
4. Added Thermal Protection	1000	3300	4300 ±30%
5. Beam Waveguide	800	5250	6050 ±30%
6. Smooth Subreflector (0.0152 cm vs. 0.254 cm) (0.006" vs. 0.010")	150	2400	2550 ±15%
7. Panel Actuators (1800 ea)	1700	16800	18500 ±20%
8. Pointing and Tracking System (vs. ±0.006°)			
0.004°	300	600	900 ±5%
0.002°	950	1740	2690 ±15%
0.001°	1700	5100	5400 ±20%
9. Seven-Element Array-Feed System*	2200	11880	14080 ±50%

* Electronic-phasing error compensation and vernier beam steering resulting in closed-loop pointing to ±0.001°, with compensation for gravity, wind, and thermal structural distortions and partial turbulence phase-front distortion recovery. This consists of seven feeds, seven masers, seven receivers, and a real-time combiner, including software.

Table 6. Estimates for 70-m Antenna Performance

	A	B	C	D	E	F	G
1	851003 RMD						
2	70METER						
3							
4	INPUTS						
5		COMPUTATIONS					
6							
7	FREQUENCY GHz			2.295	8.45	32	
8		WAVELENGTH, m		.1306285	.0354784	.0093685	
9		WAVELENGTH, in		5.142846	1.396785	.3688385	
10	rms SURFACE TOTAL ERROR, in			.024	.024	.024	
11		WAVEL. FRACTION		214.2852	58.19936	15.36827	
12		RUZE LOSS, dB		.0149355	.2024732	2.903716	
13							
14	RF EFFICIENCIES						
15							
16	W/G LOSSES			1	.984	.98	
17	DICHROIC LOSS			.978	.992	1	
18	FWD SPILLOVER			.959	.964	.97	
19	REAR SPILLOVER			.994	.997	.997	
20	ILLUMINATION			.959	.982	.98	
21	X-POLARIZATION			1	1	1	
22	PHASE			.994	.989	.98	
23	CENTRAL BLOCKAGE			.983	.988	.99	
24	m /= 1 MODES			.98	.98	.978	
25	VSWR			.991	.991	.99	
26	MESH LOSS			1	.999	.998	
27							
28		RF SUBTOTAL		.848	.873	.871	
29							
30	MECHANICAL & OTHER EFFICIENCIES						
31							
32	QUADRIPOD BLOCKAGE			.9196	.9196	.9196	
33	MFG REFL (.008")			.9996	.9948	.9285	
34	SETTING (.015")			.9987	.982	.7704	
35	MFG SUBREFLECTOR (.010")			.9994	.9919	.8905	
36	GRAVITY 30 deg (.008")			.9996	.9948	.9285	
37	THERMAL (.010")			.9994	.992	.8905	
38	WIND 20 mph (.011")			.9993	.9903	.8691	
39	ATMOSPH. TURBULENCE 30 deg			.9994	.9916	.8864	
40	POINTING ERROR +/-.002 deg			.9992	.9894	.8568	
41							
42		MECH & OTHER SUBTO		.915	.854	.320	
43							
44		SYSTEM TOTAL		.776	.746	.278	
45							
46		dB EFFICIENCY		-1.10	-1.27	-5.55	
47							
48	ERROR (EXPERIENCE), dB				0	.5	
49					-.5	-.5	
50							
51		HPBW, deg		.1155876	.0313933	.0082898	
52	POINTING ERROR, +/- deg			.003	.003	.003	
53		POINT. EFFICIENCY		.9982300	.9762311	.7021993	
54		dB POINT. LOSS		-.007694	-.104473	-1.53540	

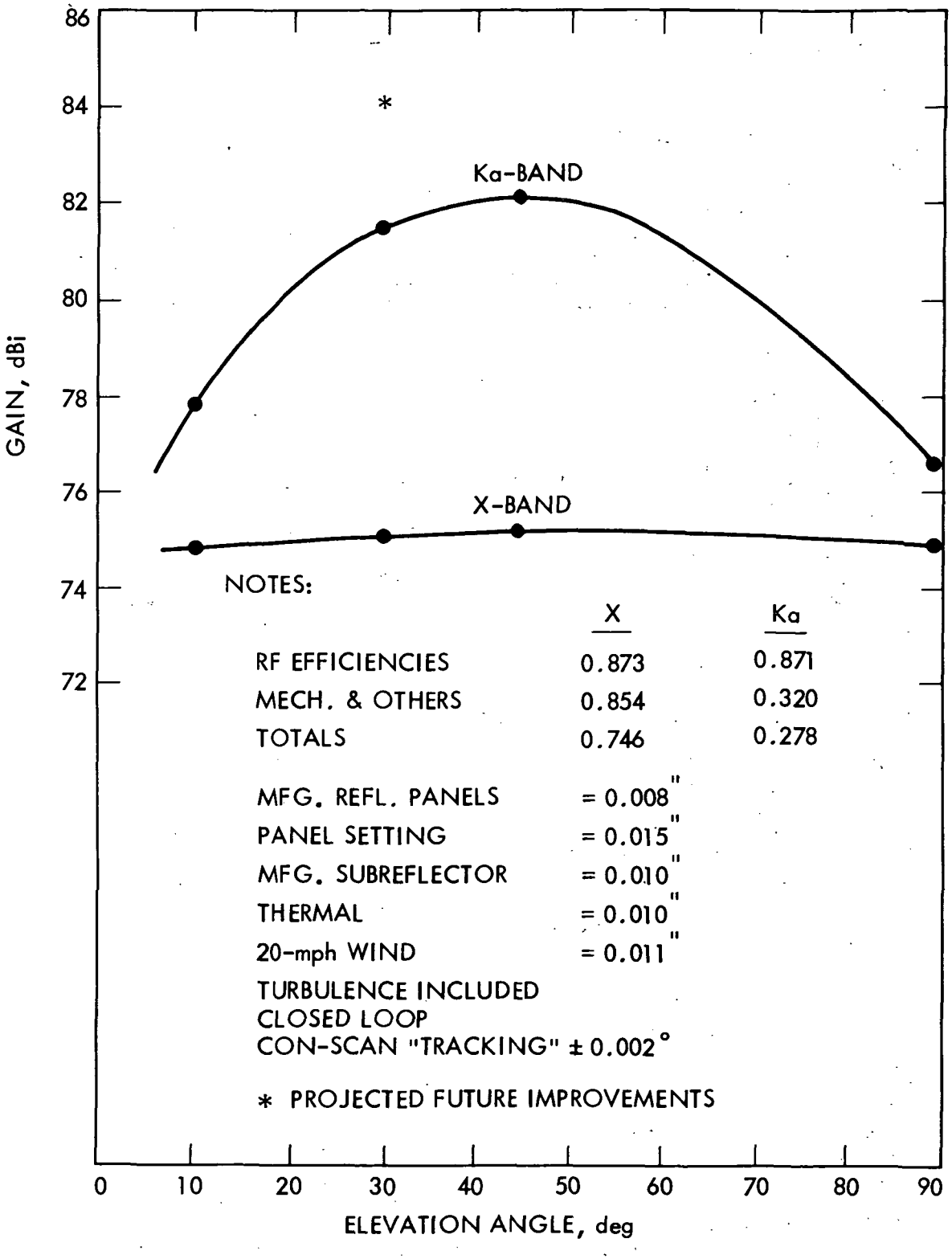

Figure 9. Antenna Performance at 64-m-to-70-m Upgrade

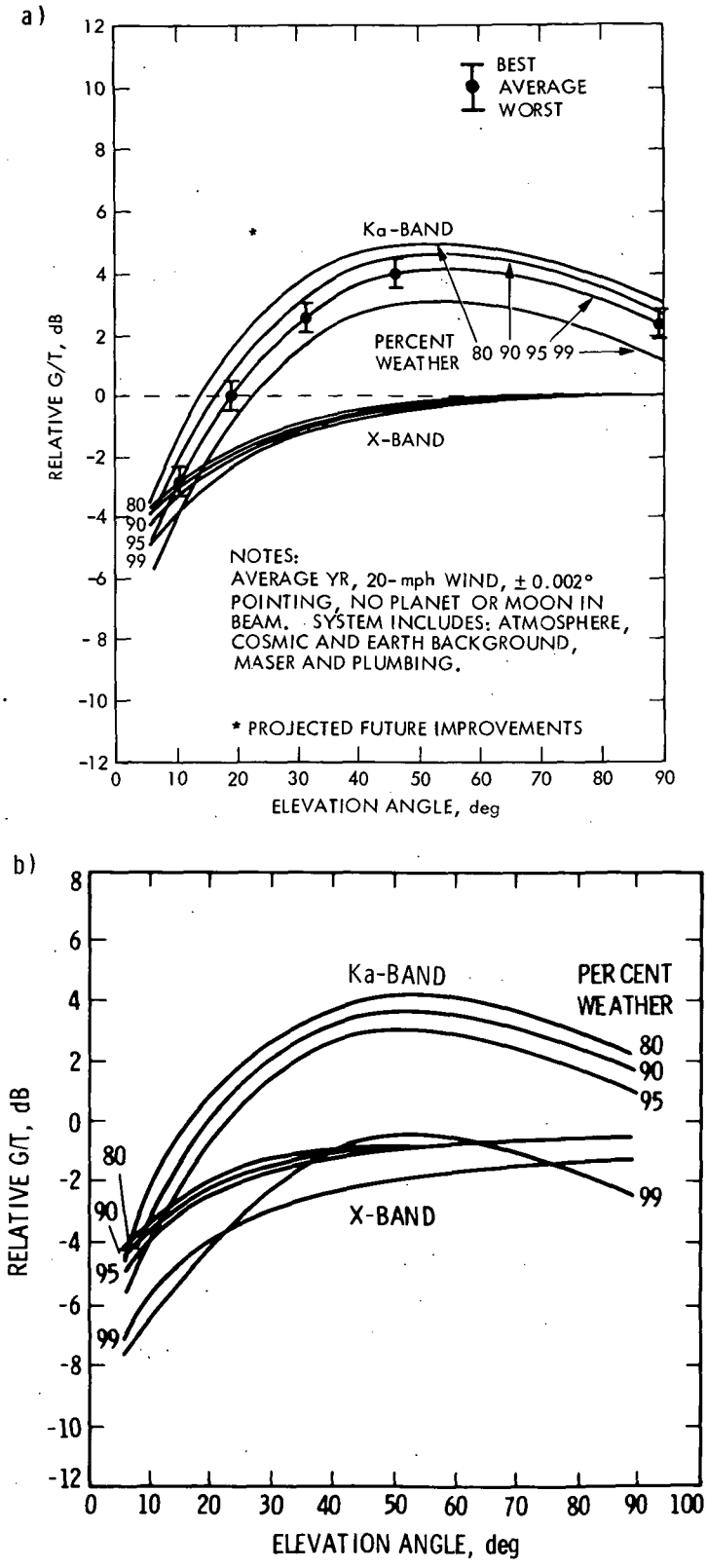

Figure 10. Ka- and X-Band G/T Performance: a) Goldstone; and b) Madrid/Canberra

angles. Other than moving to orbit or modifying the atmosphere, there is not much that can be done about the latter effect. However, the gravity sag, antenna performance degradation can be partially compensated for by either of two methods. One uses an array feed with individually controlled phasing and amplitude of each element before final signal summation. The feed array must be large enough to encompass the major fraction of the energy in the blur circle in the focal region. Alternatively, a mechanical array of independently controllable push rods on the reflector panel corners could be used to modify in real time the shape of the antenna surface as it flexes during elevation changes. In theory, the mechanical correction can fully recover the gain loss, including the residual individual panel edge diffraction losses that the electronic array feed cannot recover.

Figure 11 shows the predicted gain increases for the two different 70-m performance improvement methods. A more thorough, detailed analysis will be required to determine whether sensing of reflector surface figure effects (on the main beam gain) and electronic RF compensation, or sensing of mechanical figure departure and (compensating) displacement correction is the most cost effective approach to minimizing the gravity distortion gain losses. A combination of mechanical and electronic array techniques may be most viable.

Based upon the above scenario of 70-m antenna performance and weather effects, the design control Tables 7, 8, and 9 for the performance of the current 64-to-70-m upgrade at X-band and Ka-band and the array feed improved performance at Ka-band, respectively, are used to set the data rate that a particular spacecraft eirp can support. For performing the optimization methodology, the assumption is that increases or decreases in spacecraft eirp lead to proportionate data rate increases or decreases. Although certain system nonlinearities make this assumption not strictly true (and spacecraft data rate capabilities are generally quantized), in general it is satisfactory for comparative assessment purposes. The reference data rates related to a particular eirp are key elements in the optimization routine in the Supercalc 3 program.

C. SPACECRAFT MICROWAVE SYSTEMS

The X-band system block diagram is shown in Figure 12. The model consists of a large diameter antenna and a low-power transmitter, due to the cost of dc power. If antenna costs were simply proportional to area as the analytic model assumes, then the optimum diameter would be about 7.1 m, with an 8-W transmitter. However, any antenna over 4.5 m in diameter is required to be deployable because of the Shuttle bay diameter constraint. The approximate cost increment to go deployable is on the order of $7M. Hence, the resulting X-band design was constrained to the maximum 4.5-m antenna, but with a higher power (10 W) than the minimum level transmitter.

The Ka-band system shown in Figure 13 consists of a solid aperture antenna with an array feed in order to yield the highest efficiency solid-state power combining, in space rather than in a lossy transmission line. Also, the array feed can be outfitted with an electronic beam steering capability in order to vernier point the high-gain beam. Unconstrained by the Shuttle payload bay diameter, the optimum antenna diameter would be large in

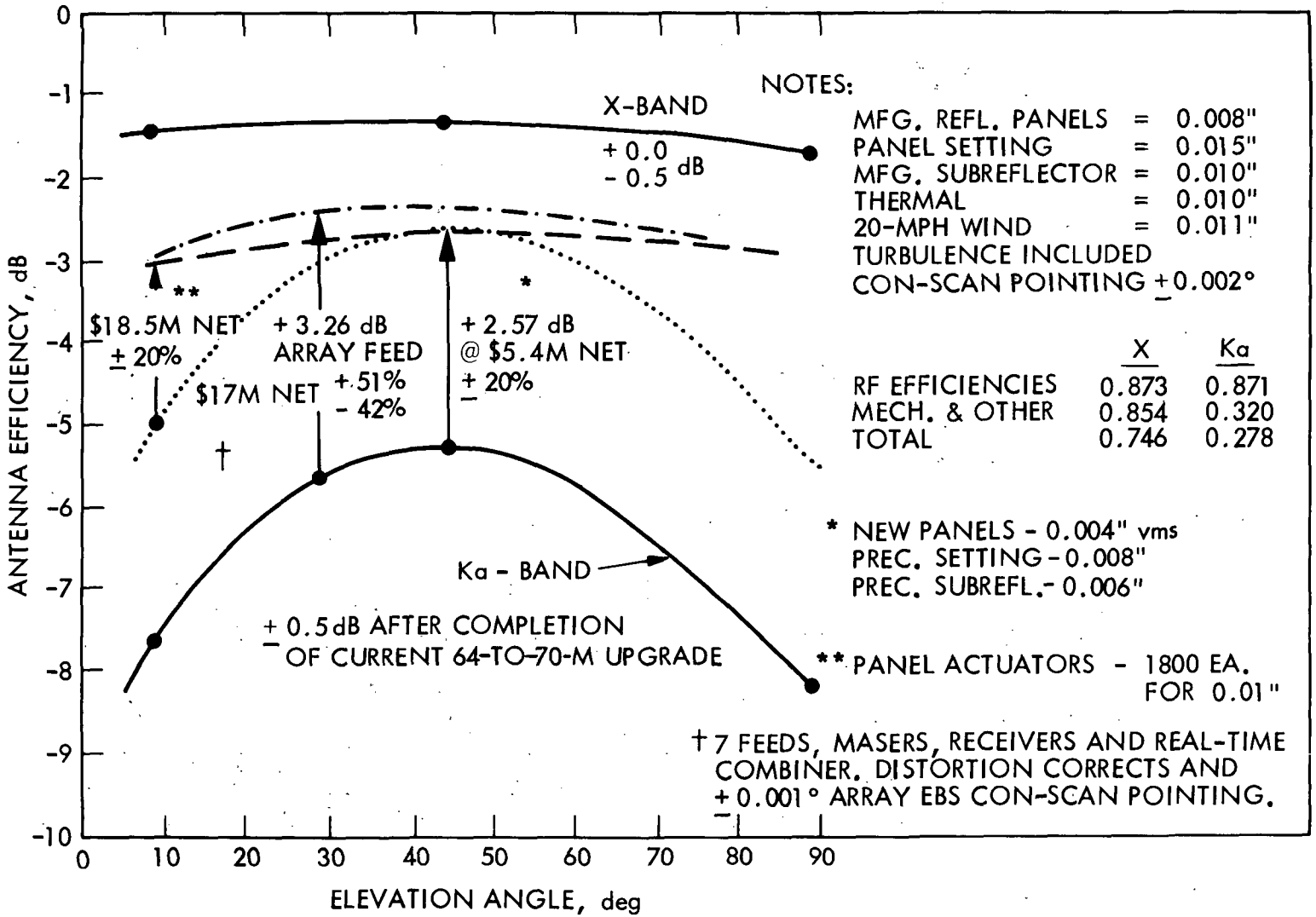

Figure 11. Proposed 70-m Antenna Efficiency Improvements

Table 7. X-Band Reference Link Performance Estimate

	A	B	C	D	E	F	G	H
1	851004RMD							
2	XKDCT-X							
3								
4	TELECOMMUNICATION DOWNLINK TELEMETRY PERFORMANCE ESTIMATES							
5								
6	MISSION: SOTP							
7	X- AND Ka-BAND SPACECRAFT							
8	CANBERRA 70 M @ MKIV UPGRADE							
9	REF: M. KOERNER DCT PROGRAM NO. 530-P ***							
10								
11	DCT AREA							
12		ITEM DESCRIPTION						
13					INPUT			
14					VALUES			(NOMINAL)
15					(NOMINAL)		NOTES	COMPUTED
16								VALUES
17		FREQUENCY, GHz			8.415			
18		WAVELENGTH, m						.0356260
19	SPACECRAFT RF POWER GENERATION PARAMETERS							
20		dc TO dc CONV. EFF.			.85			
21		dc TO RF CONV. EFF.			.406			
22		PWR AMP RF OUTPUT, W & dBm			10.00			40.00
23		S/C PRIME dc POWER, W						28.98
24		LINE & FILT. etc LOSS, dB			-.75		fraction	.84
25		RF POWER TO ANT. FEED, dBm				+0.25/-0.26 dB tol		39.25
26								
27	SPACECRAFT ANTENNA PARAMETERS							
28		CASSEGRAIN MAIN DIAMETER, m			4.5			
29		FEED ILLUM. & SPILLOVER			.87			
30		CENTER BLOCKAGE			.96			
31		STRUT & W/G BLOCKAGE			.95			
32		CROSS POLARIZATION			1			
33		SUBREFLECTOR DIFFRACTION			.93			
34		DICHROIC TRANSMITTANCE			1			
35		FEED OHMIC LOSS FACTOR			.98			
36		FEED TO BACK OF REFL.			.98			
37		GRATING LOBES LOSS FACTOR			1		NOT ARRAY FEED	
38		UNMODELED LOSSES			.97			
39		SUBTOTAL ON AXIS FEED EFFICIENCY						.687
40		SUBREFL. SURFACE rms, in			.006			.997
41		MAIN REFL. SURF. rms, in			.022			.962
42		SUBTOTAL ON AXIS HGA BEAM EFFICIENCY						.659
43								
44		HGA PEAK GAIN, dBi			+0.21/-0.22 dB tol.			50.16
45								
46	ANTENNA POINTING PARAMETERS							
47		POINTING ERROR, deg			.10			
48		POINTING LOSS, dB						-.48
49		POINTING LOSS, DECIMAL FRACTION						.896
50		EBS SCAN & QUANTZ. LOSS, dB			0		NOT ARRAY FEED	1
51		SUBTOTAL HGA EFF. AT POINTING ERROR						.590
52								
53	SPACECRAFT EFFECTIVE RADIATED POWER							
54		TOTAL EFF. HGA, POINT. & LINE LOSSES					fraction	.497
55		EIRP, dBm				88.93CHECK		88.93
56								
57	PROPAGATION PATH PARAMETERS							
58		MAX. RANGE, AU & m			11			1.646e12
59		FREE SPACE LOSS, dB						-295.275
60		CANBERRA ELEV. ANGLE, deg			30			
61		WEATHER PERCENTAGE, %			90			

Table 7. X-Band Reference Link Performance Estimate (Continued)

62		O2, H2O VAPOR, CLOUDS & RAIN LOSS, dB		INPUT>	-.07
63		TOTAL SPACE & SKY LOSS, dB			-295.35
64					
65	DSN RECEIVING ANTENNA EFFICIENCY FACTORS				
66		ANTENNA DIAMETER. m	70		
67		FEED ILLUMINATION	.982		
68		FORWARD SPILLOVER	.964		
69		REAR SPILLOVER	.997		
70		CENTRAL BLOCKAGE	.988		
71		CROSS POLARIZATION	1		
72		PHASE	.989		
73		m /= 1 MODES	.98		
74		VSWR	.991		
75		WAVEGUIDE LOSSES	.984		
76		MESH LOSS	.999		
77		DICHROIC LOSSES	.992		
78		SUBTOTAL RF EFFICIENCY			.873
79					
80		QUADRIPOD BLOCKAGE	.9196		
81		MFG. REFLECTOR, in rms	.008		.995
82		PANEL SETTING, in rms	.015		.982
83		MFG. SUBREFLECTOR, in rms	.010		.992
84		GRAVITY 30 deg, in rms	.008		.995
85		THERMAL, in rms	.010		.992
86		WIND 20 mph, in rms	.011		.990
87		ATMOS. TURBULENCE @ 30 deg	.9916		
88		TRACKING ERROR , +/- deg	.002	CONSCAN	
89		POINTING LOSS, dB & FRACT.	-.046		.989
90		SUBTOTAL MECHANICAL & OTHER EFF.			.855
91					
92		TOTAL DSN ANTENNA EFFICIENCY			.747
93					
94		DSN ANTENNA GAIN, dBi	+0.0/-0.5 dB tol.		74.54
95					
96	LOW NOISE RECEIVER SUBSYSTEM PARAMETERS				
97		MASER & PLUMBNG TEMP, deg K	8.9		
98		GROUND RADIATION, deg K	6.5		
99		COSMIC BACKGROUND, deg K	2.6		
100		CANBERRA 30deg, 90% SKY, K			3.808
101		SUBTOTAL RECEIVE SYSTEM TEMPERATURE, deg K		SLOBIN	21.808
102					
103		NOISE SPECTRAL DENSITY, dBm/Hz			-185.215
104					
105	AVAILABLE Pt/No, dB-Hz				53.34
106					
107	DATA RATE PERFORMANCE ESTIMATE				
108		*** REFERENCE DATA RATE, Hz	15789		
109		CORRESPOND. REQ'D Pt/No, dB	46.12		
110		REQ'D PERF. MARGIN, dB	2.61		
111		EXCESS MARGIN, dB			4.61
112					
113		AVAILABLE DATA RATE, Hz			45,681.5

Table 8. Ka-Band Link Performance Estimate at 70-m Upgrade Completion

	A	B	C	D	E	F	G	H
1	851030RMD							
2	XKDCT-KA		70 M DSN AUGMENTED WITH 7 ELEMENT RECEIVE ARRAY FEED					
3			AND MORE PRECISE SUBREFLECTOR, PANELS AND PANEL SETTIN					
4	TELECOMMUNICATION DOWNLINK TELEMETRY PERFORMANCE ESTIMATES							
5								
6	MISSION: SOTP							
7	X- AND Ka-BAND SPACECRAFT							
8	CANBERRA 70 M @ MKIV UPGRADE AND WITH ARRAY FEED FOR Ka-BAND							
9	REF: M. KOERNER DCT PROGRAM NO. 530-P ***							
10								
11	DCT AREA							
12		ITEM DESCRIPTION						
13					INPUT			
14					VALUES		NOTES	(NOMINAL)
15					(NOMINAL)			COMPUTED
16								VALUES
17		FREQUENCY, GHz			32			
18		WAVELENGTH, m						.0093685
19	SPACECRAFT RF POWER GENERATION PARAMETERS							
20		dc TO dc CONV. EFF.			.85			
21		dc TO RF CONV. EFF.			.247			
22		PWR AMP RF OUTPUT, W & dBm			5.00			36.99
23		S/C PRIME dc POWER, W						23.82
24		LINE & FILT. etc LOSS, dB			0	ARRAY FEED		.1
25		RF POWER TO ANT. FEED, dBm				+0.56/-0.99 dB tol		36.99
26								
27	SPACECRAFT ANTENNA PARAMETERS							
28		MAIN REFLECTOR DIAMETER, m			4.5			
29		FEED ILLUM. & SPILLOVER			.92			
30		CENTER BLOCKAGE			.94			
31		STRUT & W/G BLOCKAGE			.93			
32		CROSS POLARIZATION			1			
33		SUBREFLECTOR DIFFRACTION			.96			
34		DICHROIC TRANSMITTANCE			.97			
35		FEED OHMIC LOSS FACTOR			.98			
36		FEED TO BACK OF REFL.			1		ARRAY FEED	
37		GRATING LOBES LOSS FACTOR			.97			
38		UNMODELED LOSSES			.97			
39		SUBTOTAL ON AXIS FEED EFFICIENCY						.691
40		SUBREFL. SURFACE rms, in			.003			.990
41		MAIN REFL. SURF. rms, in			.008			.928
42		SUBTOTAL ON AXIS HGA BEAM EFFICIENCY						.634
43								
44		HGA PEAK GAIN, dBi			+ 0.21/-0.28 dB tol.			61.60
45								
46	ANTENNA POINTING PARAMETERS							
47		POINTING ERROR, deg			.025		EBS	
48		POINTING LOSS, dB					EBS	
49		POINTING LOSS, DECIMAL FRACTION				ONLY EBS SCAN LOSS		1
50		EBS SCAN & QUANTZ. LOSS, dB			-.640	FOR 0.1 deg SCAN		.863
51		SUBTOTAL HGA EFF. AT POINTING ERROR						.548
52								
53	SPACECRAFT EFFECTIVE RADIATED POWER							
54		TOTAL EFF. HGA, POINT. & LINE LOSSES						.548
55		EIRP, dBm						97.95
56								
57	PROPAGATION PATH PARAMETERS							
58		MAX. RANGE AU & m			11			1.646e12
59		FREE SPACE LOSS, dB						-306.877
60		CANBERRA ELEV. ANGLE, deg			30			
61		WEATHER PERCENTAGE, %			90			

Table 8. Ka-Band Link Performance Estimate at 70-m Upgrade Completion (Continued)

62	O2, H2O VAPOR, CLOUDS & RAIN LOSS, dB		INPUT>		-.574
63	TOTAL SPACE & SKY LOSS, dB				-307.451
64					
65	DSN RECEIVING ANTENNA EFFICIENCY FACTORS				
66	ANTENNA DIAMETER. m	70			
67	FEED ILLUMINATION	.98			
68	FORWARD SPILLOVER	.97			
69	REAR SPILLOVER	.997			
70	CENTRAL BLOCKAGE	.99			
71	CROSS POLARIZATION	1			
72	PHASE	.98			
73	m /= 1 MODES	.978			
74	VSWR	.99			
75	WAVEGUIDE LOSSES	.98			
76	MESH LOSS	.998			
77	DICHROIC LOSSES	1			
78	SUBTOTAL RF EFFICIENCY				.871
79					
80	QUADRIPOD BLOCKAGE	.9196			
81	MFG. REFLECTOR, in rms	.008			.928
82	PANEL SETTING, in rms	.015			.770
83	MFG. SUBREFLECTOR, in rms	.010			.890
84	GRAVITY 30 deg, in rms	.008			.928
85	THERMAL, in rms	.010			.890
86	WIND 20 mph, in rms	.011			.869
87	ATMOS. TURBULENCE @ 30 deg	.8864			
88	TRACKING ERROR , +/- deg	.002	CONSCAN		
89	POINTING LOSS, dB & FRACT.	-.672			.857
90	SUBTOTAL MECHANICAL & OTHER EFF.				.319
91					
92	TOTAL DSN ANTENNA EFFICIENCY				.278
93					
94	DSN ANTENNA GAIN, dBi		+/- 0.5 dB tol.		81.85
95					
96	LOW NOISE RECEIVER SUBSYSTEM PARAMETERS				
97	MASER & PLUMBNG TEMP, deg K	7.3			
98	GROUND RADIATION, deg K	6.5			
99	COSMIC BACKGROUND, deg K	2.2			
100	CANBERRA 30deg, 90% SKY, K				35.057
101	SUBTOTAL RECEIVE SYSTEM TEMPERATURE, deg K			SLOBIN	51.057
102					
103	NOISE SPECTRAL DENSITY, dBm/Hz				-181.521
104					
105	AVAILABLE Pt/No, dB-Hz				53.87
106					
107	DATA RATE PERFORMANCE ESTIMATE				
108	*** REFERENCE DATA RATE, Hz	15789			
109	CORRESPOND. REQ'D Pt/No, dB	46.12			
110	REQ'D PERF. MARGIN, dB	3	< MY WAG		
111	EXCESS MARGIN, dB				4.75
112					
113	AVAILABLE DATA RATE, Hz				47,131.2

Table 9. Ka-Band Improved Link Performance Estimate

	A	B	C	D	E	F	G	H
1	851004RMD							
2	XKDCT-K							
3								
4	TELECOMMUNICATION DOWNLINK TELEMETRY PERFORMANCE ESTIMATES							
5								
6	MISSION: SOTP							
7	X- AND Ka-BAND SPACECRAFT							
8	CANBERRA 70 M @ MKIV UPGRADE							
9	REF: M. KOERNER DCT PROGRAM NO. 530-P ***							
10								
11	DCT AREA							
12		ITEM DESCRIPTION			INPUT VALUES (NOMINAL)		NOTES	(NOMINAL) COMPUTED VALUES
16								
17		FREQUENCY, GHz			32			
18		WAVELENGTH, m						.0093685
19	SPACECRAFT RF POWER GENERATION PARAMETERS							
20		dc TO dc CONV. EFF.			.85			
21		dc TO RF CONV. EFF.			.247			
22		PWR AMP RF OUTPUT, W & dBm			5.00			36.99
23		S/C PRIME dc POWER, W						23.82
24		LINE & FILT. etc LOSS, dB			.00	ARRAY FEED, fract		1
25		RF POWER TO ANT. FEED, dBm				+0.56/-0.99 dB tol		36.99
26								
27	SPACECRAFT ANTENNA PARAMETERS							
28		MAIN REFLECTOR DIAMETER, m			4.5			
29		FEED ILLUM. & SPILLOVER			.92			
30		CENTER BLOCKAGE			.94			
31		STRUT & W/G BLOCKAGE			.93			
32		CROSS POLARIZATION			1			
33		SUBREFLECTOR DIFFRACTION			.96			
34		DICHROIC TRANSMITTANCE			.97			
35		FEED OHMIC LOSS FACTOR			.98			
36		FEED TO BACK OF REFL.			1		ARRAY FEED	
37		GRATING LOBES LOSS FACTOR			.97			
38		UNMODELED LOSSES			.97			
39		SUBTOTAL ON AXIS FEED EFFICIENCY						.691
40		SUBREFL. SURFACE rms, in			.003			.990
41		MAIN REFL. SURF. rms, in			.008			.928
42		SUBTOTAL ON AXIS HGA BEAM EFFICIENCY						.634
43								
44		HGA PEAK GAIN, dBi				+0.21/-0.28 dB tol		61.60
45								
46	ANTENNA POINTING PARAMETERS							
47		POINTING ERROR, deg			.025		EBS	
48		POINTING LOSS, dB					EBS	
49		POINTING LOSS, DECIMAL FRACTION				ONLY EBS SCAN LOSS		1
50		EBS SCAN & QUANTZ. LOSS, dB			-.640	FOR 0.1 deg SCAN		.863
51		SUBTOTAL HGA EFF. AT POINTING ERROR						.548
52								
53	SPACECRAFT EFFECTIVE RADIATED POWER							
54		TOTAL EFF. HGA, POINT. & LINE LOSSES					fraction	.548
55		EIRP, dBm						97.95
56								
57	PROPAGATION PATH PARAMETERS							
58		MAX. RANGE AU & m			11			1.646e12
59		FREE SPACE LOSS, dB						-306.877
60		CANBERRA ELEV. ANGLE, deg			30			
61		WEATHER PERCENTAGE, %			90			

Table 9. Ka-Band Improved Link Performance Estimate (Continued)

62	O2, H2O VAPOR, CLOUDS & RAIN LOSS, dB			INPUT>	-.574
63	TOTAL SPACE & SKY LOSS, dB				-307.451
64					
65	DSN RECEIVING ANTENNA EFFICIENCY FACTORS				
66	ANTENNA DIAMETER. m	70			
67	FEED ILLUMINATION	.98			
68	FORWARD SPILLOVER	.97			
69	REAR SPILLOVER	.997			
70	CENTRAL BLOCKAGE	.99			
71	CROSS POLARIZATION	1			
72	PHASE	.98			
73	m /= 1 MODES	.978			
74	VSWR	.99			
75	WAVEGUIDE LOSSES	.98			
76	MESH LOSS	.998			
77	DICHROIC LOSSES	1			
78	SUBTOTAL RF EFFICIENCY				.871
79					
80	QUADRIPOD BLOCKAGE	.9196			
81	MFG. REFLECTOR, in rms	.004		NEW PANEL	.982
82	PANEL SETTING, in rms	.008		PRECISION	.928
83	MFG. SUBREFLECTOR, in rms	.006		NEW	.959
84	GRAVITY 30 deg, in rms	.002		ARRAY FED	.995
85	THERMAL, in rms	.002		ARRAY FED	.995
86	WIND 20 mph, in rms	.002		ARRAY FED	.995
87	ATMOS. TURBULENCE @ 30 deg	.888		SOME COMPENSATION	
88	TRACKING ERROR , +/- deg	.001		ARRAY CONSCAN	
89	POINTING LOSS, dB & FRACT.	-.167			.962
90	SUBTOTAL MECHANICAL & OTHER EFF.				.677
91					
92	TOTAL DSN ANTENNA EFFICIENCY				.590
93					
94	DSN ANTENNA GAIN, dBi	+0.0/-1.5 dB tol.			85.12
95					
96	LOW NOISE RECEIVER SUBSYSTEM PARAMETERS				
97	MASER & PLUMBNG TEMP, deg K	7.3			
98	GROUND RADIATION, deg K	6.5			
99	COSMIC BACKGROUND, deg K	2.2			
100	CANBERRA 30deg, 90% SKY, K				35.057
101	SUBTOTAL RECEIVE SYSTEM TEMPERATURE, deg K			SLOBIN	51.057
102					
103	NOISE SPECTRAL DENSITY, dBm/Hz				-181.521
104					
105	AVAILABLE Pt/No, dB-Hz				57.14
106					
107	DATA RATE PERFORMANCE ESTIMATE				
108	*** REFERENCE DATA RATE, Hz	15789			
109	CORRESPOND. REQ'D Pt/No, dB	46.12			
110	REQ'D PERF. MARGIN, dB	3	< MY WAG		
111	EXCESS MARGIN, dB				8.02
112					
113	AVAILABLE DATA RATE, KHz				100.0

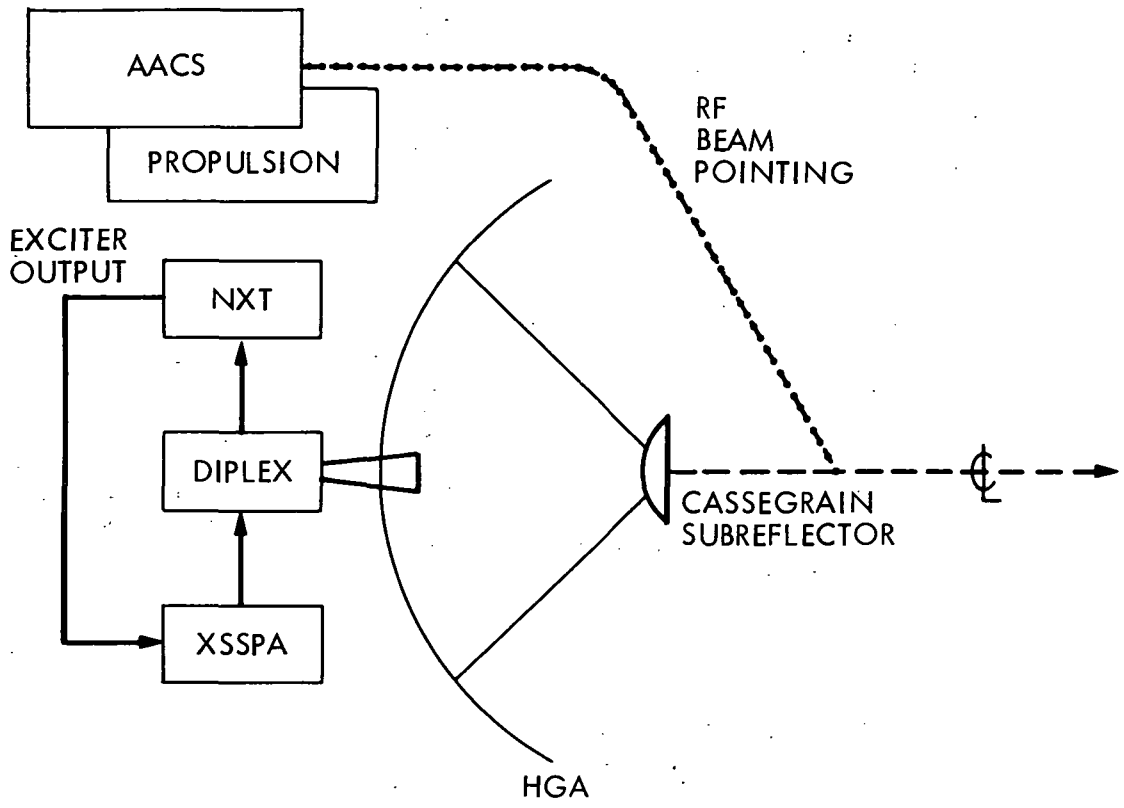

NXT = NASA X-BAND TRANSPONDER

XSSPA = X-BAND SOLID-STATE POWER AMPLIFIER

HGA = HIGH-GAIN ANTENNA

AACS = ATTITUDE AND ARTICULATION CONTROL SYSTEM

Figure 12. Spacecraft X-Band System

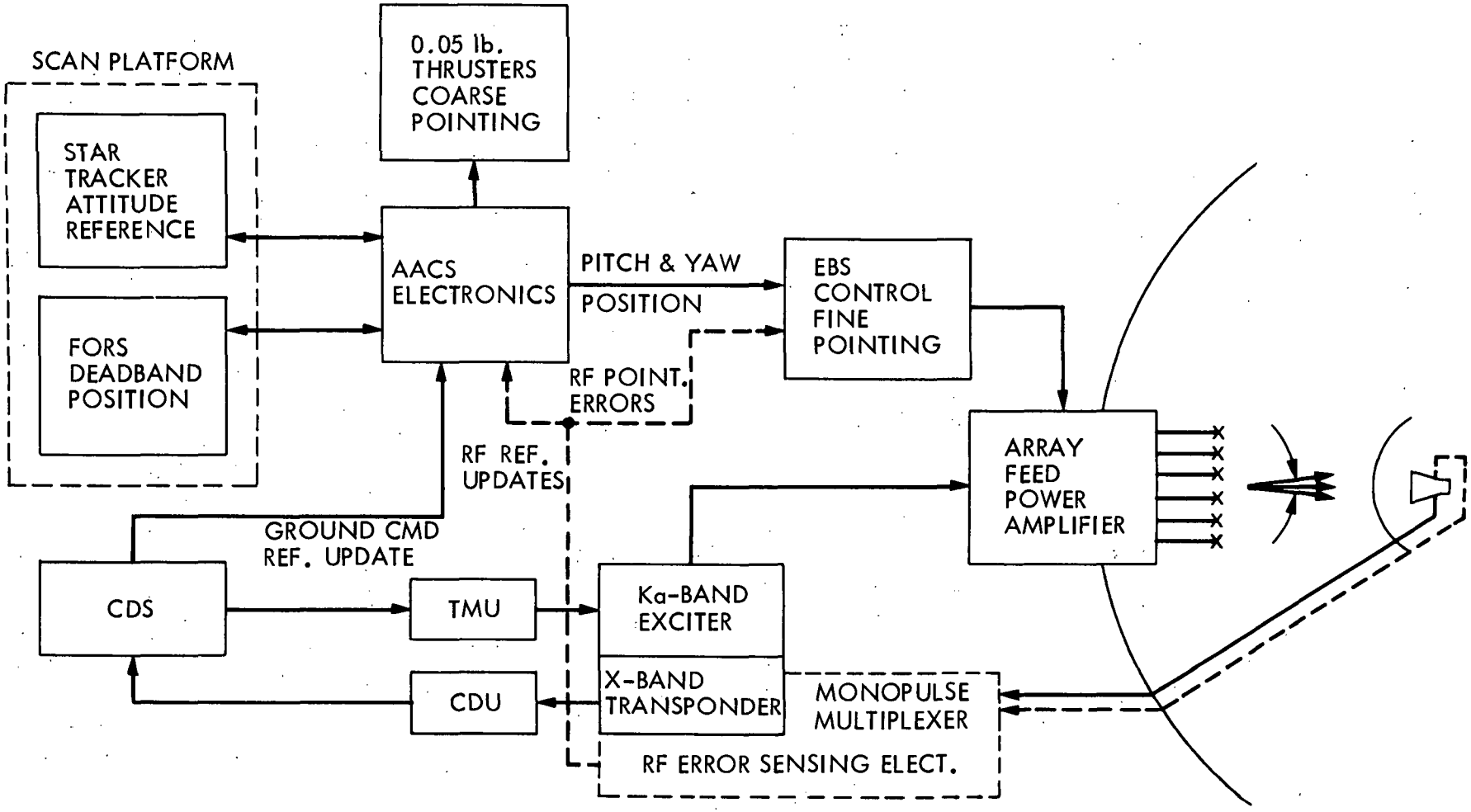

Figure 13. Spacecraft Ka-Band System

order to minimize the dc power cost. However, again due to the $7M added cost for a deployable aperture, a smaller, fixed aperture antenna (4.5 m) was selected.

The transmission line, pointing and scanning, and aperture efficiencies (relative to a uniformly illuminated aperture) of the various configuration options considered for power amplifier and antennas at X- and Ka-band are shown in Table 10 (private communication from J. Boreham and M. Gatti). The study selected a conventional Cassegrain configuration at X-band and an array-fed power amplifier with electronic beam steering at Ka-band. The table gives only the nominal performance values. The study assumed tolerances of ±10% on transmission line losses and +3% and -4% on aperture efficiencies.

D. OPTICAL FREQUENCY SPACECRAFT

The optical system spacecraft block diagram shown in Figure 14 consists of a reflective optics telescope aboard the spacecraft, vernier pointed by orthogonal mirrors near the focal region of the telescope. Coarse pointing is achieved either by pointing the entire spacecraft to which the telescope is attached or, alternatively, motor-driven gimbals are employed to move the telescope relative to the spacecraft bus. The optical vernier pointing is also used to accomplish the point ahead that is required to offset the aberration resulting from the finite speed of light, the narrow beamwidth, and the relative motion of the spacecraft and Earth terminal.

The essential elements of a concept for an optical receiving station in orbit around the Earth are shown in a sketch for a technology development scaled experiment in Figure 15. They consist of a large-diameter photon bucket collector in the Space Station complex and an uplink laser mounted to a small telescope. The received optical telemetry data would be relayed via the TDRS or TDAS networked with NASCOM to JPL.

The off-Earth location of the optical receiving terminal is based on the design approach of minimizing the effects of weather outages. Site diversity of surface-based telescopes could be employed to combat the effects of weather at any one viewing site, but the seeing and background conditions are still much inferior to space-based telescopes. However, due to the low orbit altitude, the orbiting telescope is occulted about 50% of the time. A more desirable location would be geosynchronous orbit (GEO). (A system trade study between poorer but more continuous and excellent but only 50% continuous visibility is recommended.)

Initially, the largest conceivable (20-m diameter) photon bucket was arbitrarily selected in order to minimize the spacecraft costs. However, this resulted in the optical Earth terminal being so large as to require an entire Shuttle launch (∿$140M). Additionally, the cost of EVA astronaut time for assembling, checking out, and aligning the telescope initially, and then operating and maintaining it after installation, was taken to be $80,000/hr (private communication from D. Pivirotto). These two expenses raised the total cost by an exceptional amount. Therefore, a more modest 4.5-m diameter photon bucket was selected to permit ground assembly and to occupy only one-third of a shuttle-bay launch manifest. Table 11 shows the assumed Space Station optical terminal costs.

Table 10. Spacecraft Antenna Performance Projected Estimates

Item	Feed Configuration: X-Focal Point	X-Cass.	Ka-Cass.	X-EBS	Ka-EBS
1. Feed Illumination & Spillover Assumes high efficiency feeds & shaped reflectors	.83	.87	.91	.90	.92
2. Center Blockage including LGA: EBS blockage dominated by Array Feed shadow on maindish	.98	.96	.98	.92	.94
3. Strut/WG Blockage	.92	.95	.93	.93	.93
4. Cross Polarization	.97	1.0	1.0	1.0	1.0
5. Subreflector Diffraction	NA	.93	.94	.95	.96
6. Subreflector Dichroic Loss	NA	NA	.97	.98	.97
7. Feed I^2R	.98	.98	.98	.98	.98
8. Feed WG (Feed to Back of Reflector)	.93	.98	.93	NA	NA
9. Grating Lobes	NA	NA	NA	.98	.97
10. Unmodeled Losses	.97	.97	.97	.97	.97
TOTAL ON-AXIS FEED EFFICIENCY	.641	.687	.668	.667	.690
11. Subreflector Surface X=.006", Ka=.003"	NA	.99	.99	.99	.99
12. Main Reflector Surface X=.022", Ka=.008"	.96	.96	.92	.96	.92
TOTAL ON-AXIS EFFICIENCY	.615	.653	.608	.634	.628
13. Pointing Error Loss -dB at .10° for both X and Ka	0.5 (.89)	0.5 (.89)	0.5 (.89)	NA	NA
14. EBS Scan and Quantization Losses -dB at .10° for both X and Ka	NA	NA	NA	.17 (.96)	.64 (.86)
TOTAL HGA EFFICIENCY AT MAX. POINT. ERROR	.547	.581	.541	.608	.540
15. Transmission Loss (RF Bay to HGA) -dB Assumes Ka-Cassegrain PA's behind HGA	0.7 (.85)	0.7 (.85)	0.8 (.83)	NA	NA
TOTAL HGA EFF. REF. TO PA	.465	.494	.449	.608	.540

*Assumes 4.5m Rigid Reflector

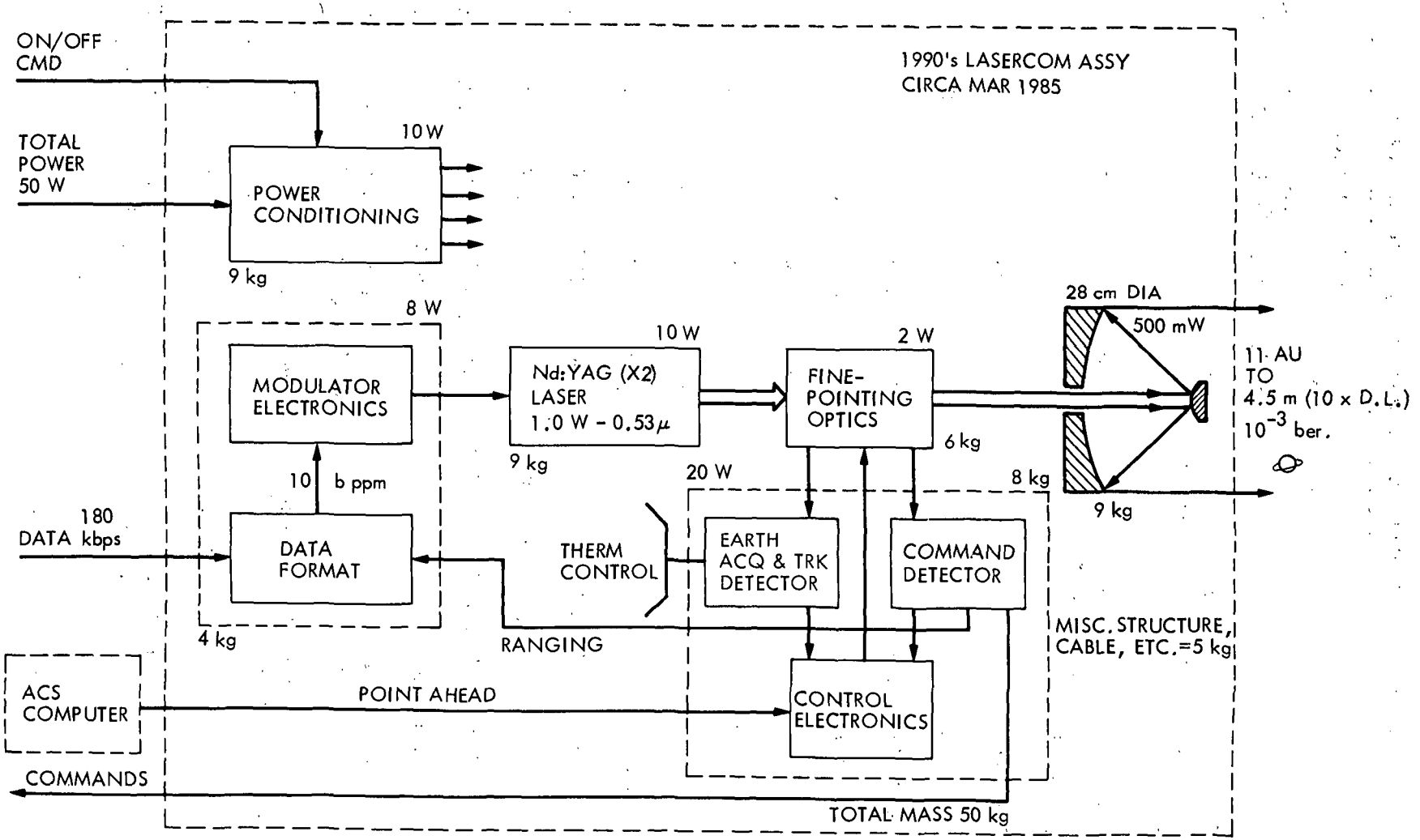

Figure 14. Spacecraft Optical Frequency System

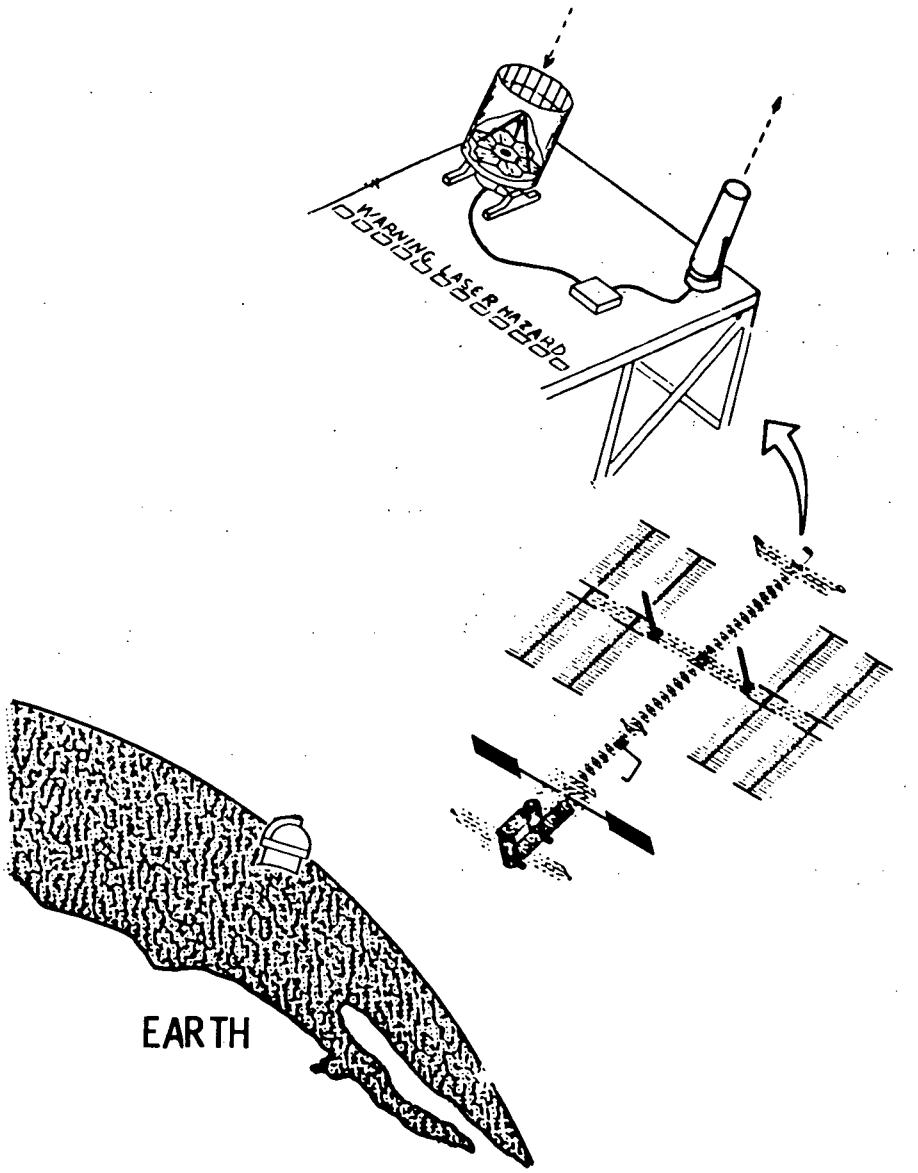

Figure 15. Optical System Earth Terminal Scaled Experiment

Table 11. Optical Terminal Cost Estimate Aboard Space Station

	NRE
4.5m PHOTON BUCKET PRIMARY (SEGMENTED/ACTUATED)	$ 3 M
SPACE STATION DECOUPLING/GIMBAL ASSEMBLY	3
MOMENTUM WHEEL ASSEMBLY	6
GYRO PACKAGE	3
FINE POINTING/DETECTOR ASSEMBLY	10
TELEMETRY ELECTRONICS	5
RANGING ELECTRONICS	5
SPACE STATION AND TDRS INTERFACES	10
50cm UPLINK TELESCOPE	1
FOCAL PLANE FINE POINTING/DETECTOR ASSEMBLY	10
MOUNTING/GIMBALS/STEERING	2
10-W LASER (>100 bps)	10
MODULATOR	2
NAVIGATION ELECTRONICS	5
INTEGRATION ABOARD SPACE STATION COMPLEX	20
ONE-THIRD SHUTTLE LAUNCH TO TRANSFER ASSEMBLY TO LEO	46
	141 M $^{+50}_{-30}$ %

Although the study was to assess all of the aspects of spacecraft telecommunications (which include not only downlink telemetry, but also uplink commanding, metric tracking, and radio science), only downlink telemetry was principally investigated. However, in the optical arena, it came to light that techniques of astrometric tracking could yield data very quickly (on the order of a few hours, as compared to many hours for VLBI) for navigation, the angles between celestial objects and the spacecraft downlink laser, in the desired reference frame at tens of picoradian-level accuracy.

The elements of cost will be discussed in the next section, along with the results of running these input parameters through the cost models.

SECTION IV

COSTING METHODS, RESULTS, AND PERFORMANCE COMPARISON

A. COSTING METHODS

The spacecraft telecommunications-related costs consist of equipment acquisition, dc power, mass transport, and spacecraft integration. The estimates include both nonrecurring (NRE) and recurring engineering (RE) costs in the equipment costs. The NRE is estimated on the basis of resources required to achieve OAST technology readiness level 6 -- "Prototype/ Engineering model tested in relevant environment" [Ref. 11]. The NRE is amortized over the quantity of applicable missions in a chosen set. In this study, the quantity was four (agreement by study team members).

Recurring engineering costs were modeled by a constant part and a part proportional to either power or area (if known), and further increased by the spares factor, 0.3 in this case (consensus by team).

For the attitude control and articulation and propulsion costs associated with the pointing of the high-gain antenna (in order to achieve the gain), the mass, power drain, and equipment costs were apportioned on a fractional basis -- 20% was used for gain achievement (the author's estimate).

For the data storage, 66% was used (author's estimate). While 88% was used for the portion of the data compression system mass, cost, and power that was attributed to the return of planetary data (author's estimate). These percentages are strictly estimates and have no basis in quantitative determination. One could think of better methods of apportioning costs, such as percent of time allocated to data storage during occultations (if such mission design details were known).

The microwave system costs were determined from the bottom up, by starting with individual major components such as a transponder or power amplifier and adding the costs of other elements of the system, antenna, exciter, etc. The individual component costs included the overhead of staff to specify and procure the components. A spacecraft integration cost (author's estimate) was added to the total, suitably weighted (author's estimate) to reflect the maturity and complexity of the particular option.

A comparable source of component costing data did not exist at JPL for the optical system. A top-down costing was done by utilizing an industry contractor cost estimate for similar equipment (private communication from J. Lesh).

A Supercalc 3 spreadsheet program was written to collect the spacecraft model costs and to permit sensitivity examinations or "what if's" on changing the parameters of the different frequency models. Table 12 shows an example of a set of optimistic, nominal and pessimistic parameters for determining RE costs at X-band, and Figure 16 shows the results of varying the dc-to-RF conversion efficiency, the cost rate of dc power, and the effect of the total number of bits to be returned.

Table 12. X-Band Optimum Spacecraft EIRP Cost Analysis Coefficients

COEFFICIENTS			
PESSIMISTIC	NOMINAL	OPTIMISTIC	
q_1 = \$120,000/kg	\$80,000/kg	\$36,000/kg	- TRANSPORTATION
k_1 = 2.3 W/kg	2.205 W/kg	2.1 W/kg	- RTG SPECIFIC MASS
q_2 = \$240,000/W	\$200,000/W	\$160,000/W	- RTG POWER COST
η_r = 0.83	0.85	0.87	- dc-dc EFFICIENCY
η_t = 0.3	0.4	0.5	- dc-RF EFFICIENCY
k_2 = 5.1 kg/m^2	3.0 kg/m^2	1.5 kg/m^2	- ANTENNA DENSITY
q_3 = \$750,000/m^2	\$530,000/m^2	\$450,000/m^2	- ANTENNA AREA COST
η_a = 0.5	0.55	0.65	- ANTENNA APERTURE EFFICIENCY
K = \$6M	K = \$4M	K = \$3.5M	- "INTEGRATION" COSTS

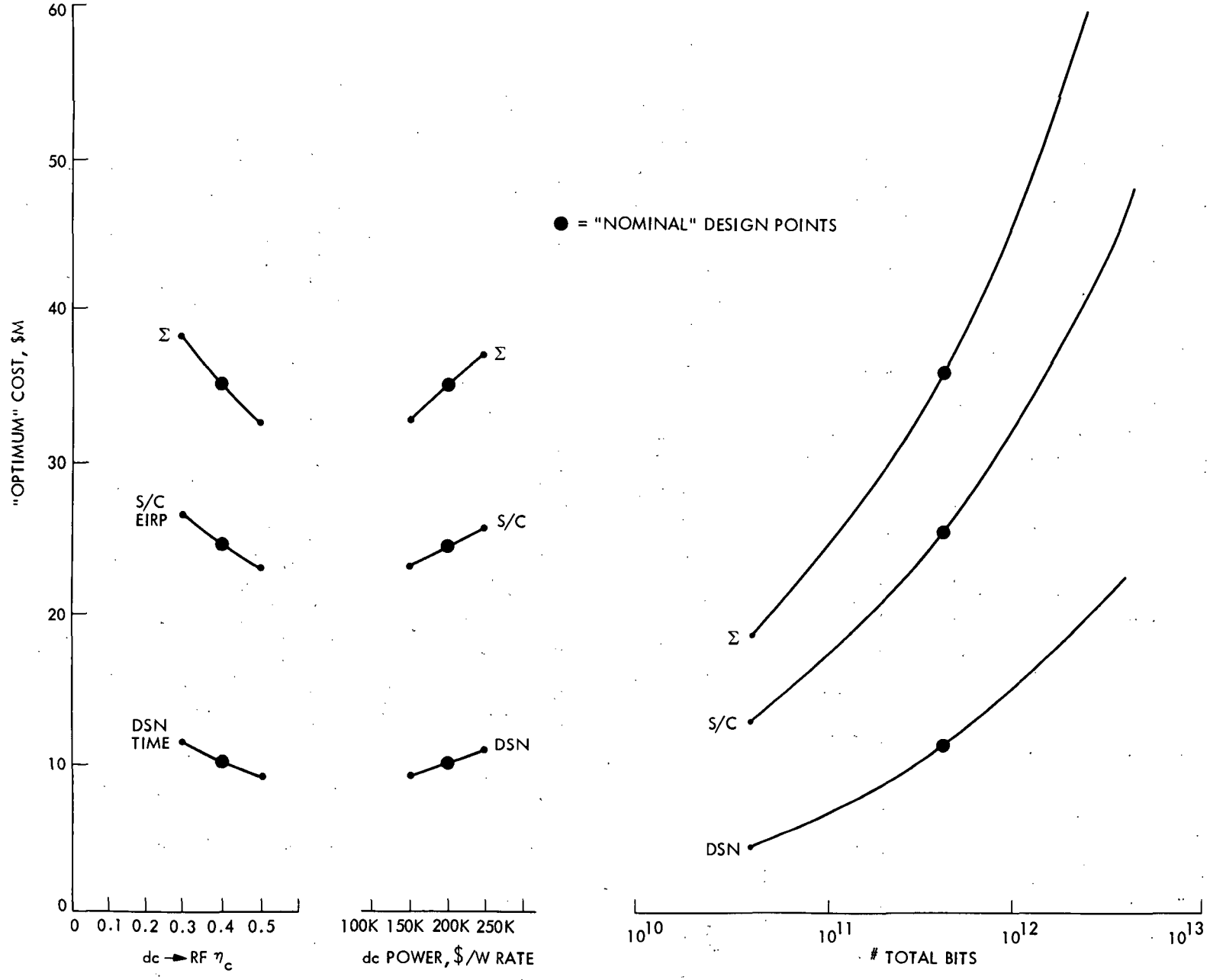

Figure 16. SOTP X-Band Parameter Sensitivity

The basic cost program had two parts. One, unconstrained, assumed the model coefficients applied over all possibilities and proceeded to determine the analytic optimum or minimum cost. The second part was fixed by input selection of transmitter power and antenna diameter and was independently set to determine the system cost, which provided a check on the first part (when its solution parameters were used as input). This also provided a means for readily determining the magnitude of the penalty for off-optimum selections.

An example of the unconstrained analytic solution is shown in Figure 17, which displays the spacecraft costs as a function of spacecraft transmitter power output with different eirp's as parameters for the various curves. The locus of minimum costs is then used as input to Figure 18, which shows the combined spacecraft and ground system costs as a function of the spacecraft eirp, with different total numbers of bits of data to be returned as a parameter.

To the above costs must be added the amortized NRE and RE for the DSN antennas or the Space Station terminal in the case of the optical system, as these were not built into the Supercalc 3 program.

B. RESULTS

Figure 19 shows the resulting costs provided by the models for four options. The options are the baseline upgraded X-band system, the Ka-band system at the completion of the currently proposed 70-m upgrade, the 70-m Ka-band system performance after the improvements are in place, and the optical system costs.

Cost elements are segregated into the four categories of spacecraft and ground recurring and nonrecurring engineering in Figure 20. The recurring engineering costs include the spares cost contribution of 30%. The displayed costs are for a single mission of the set of four. Consequently, the displayed nonrecurring engineering costs for both spacecraft and ground are 1/4 of the actual totals due to amortization over a four mission set. The error ranges shown on the plotted data represent an approximate rss of the total uncertainties (author's estimates).

The ground operations costs for the microwave systems decrease for each option compared to the X-band reference. This is due to the higher data rates, as shown in Figure 21, that can be supported by the higher frequency options. With the exception of the optical system, the spacecraft RE is approximately the same for Ka- or X-band systems. The ground operations cost savings are dramatic, but are achieved by having to increase both the NRE for the spacecraft and the DSN. However, the savings accumulate faster than the spacecraft costs grow, for a small net cost savings to NASA.

The optical system cost is dominated by the procurement cost, the transportation cost, and the installation cost for the photon bucket aboard the Space Station. The spacecraft optical system RE cost is larger than the microwave equipment RE cost, but the error bars overlap.

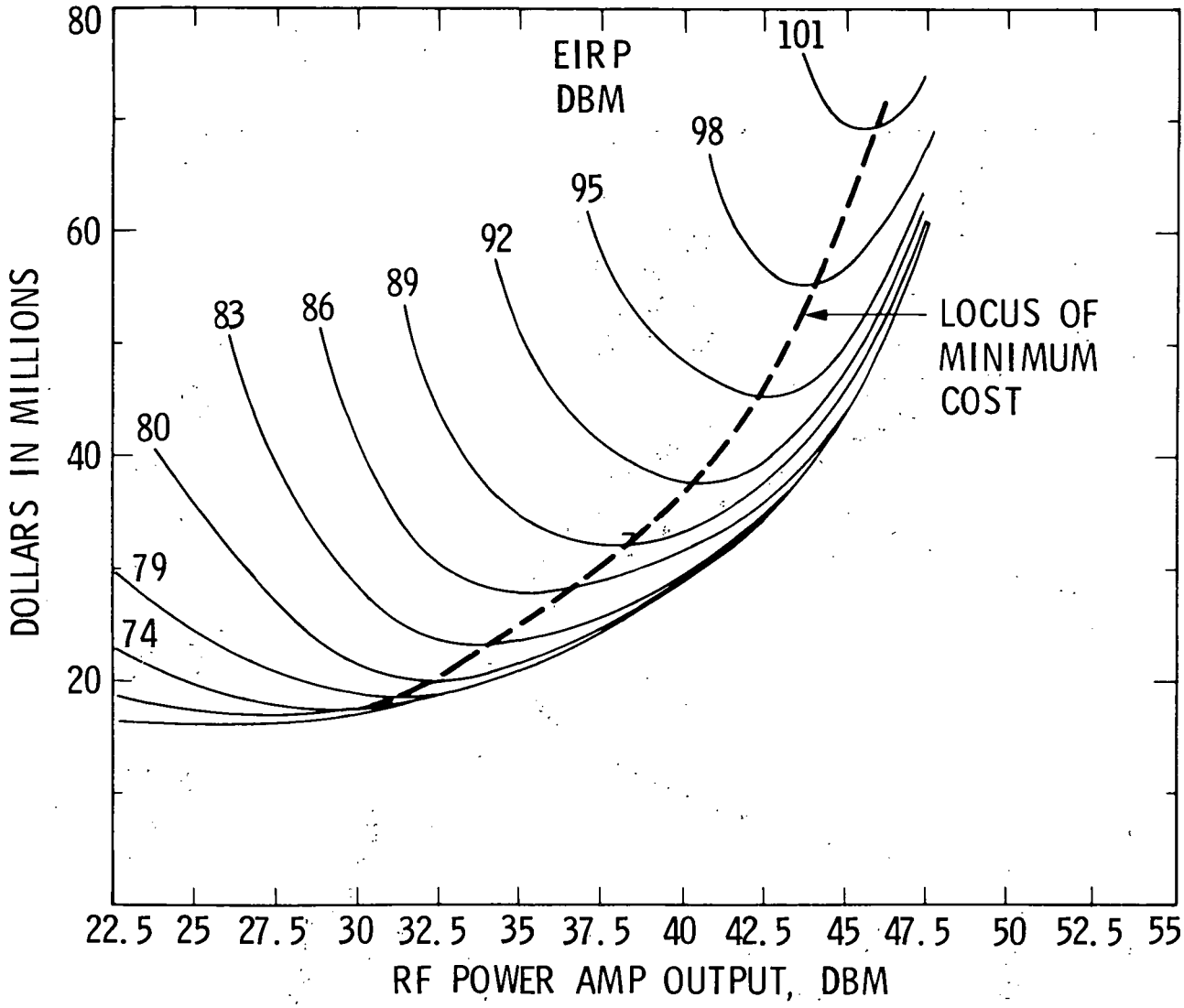

Figure 17. Minimum Cost Gain-Power Product at X-Band

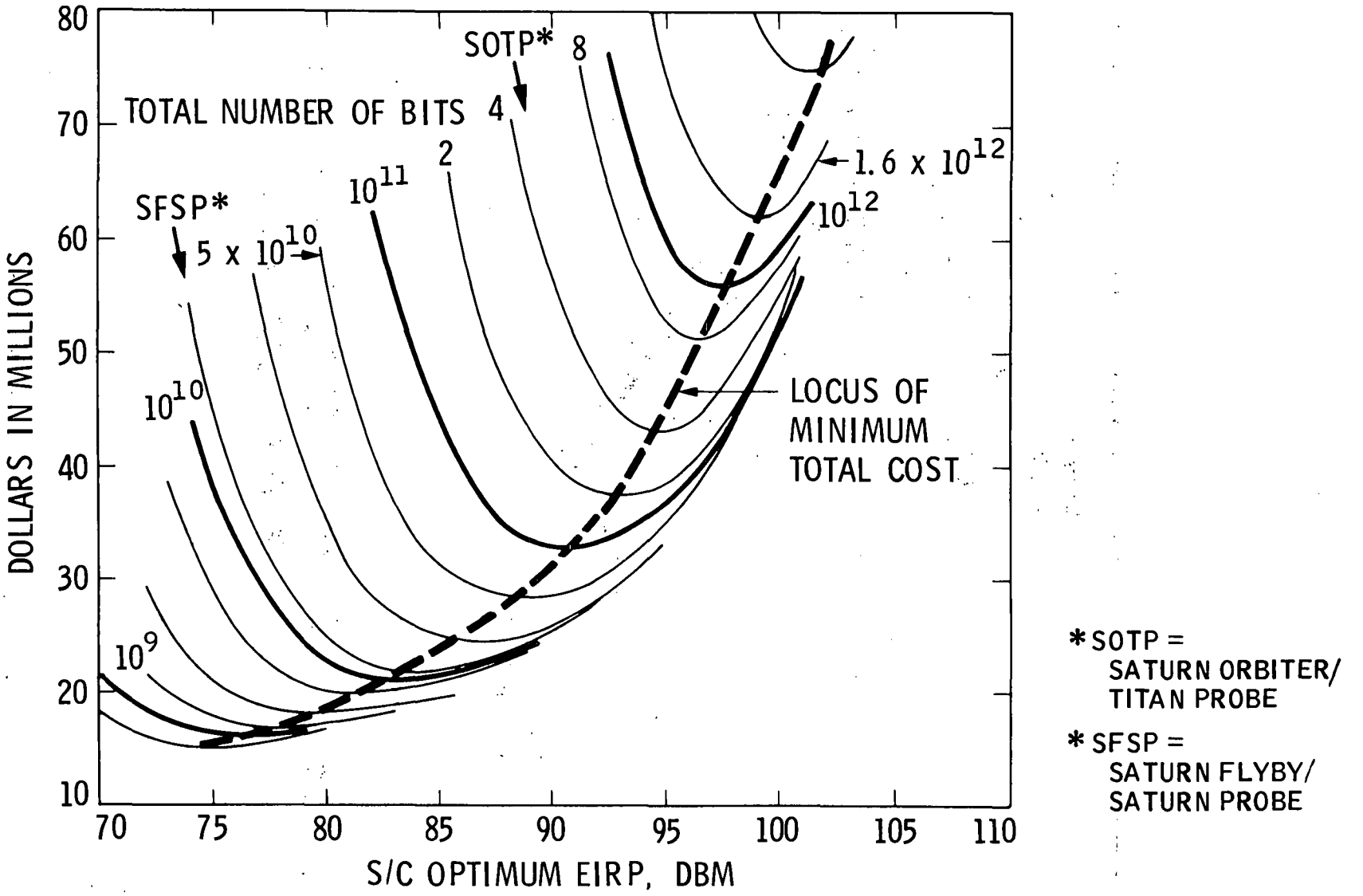

Figure 18. Minimum Information Cost

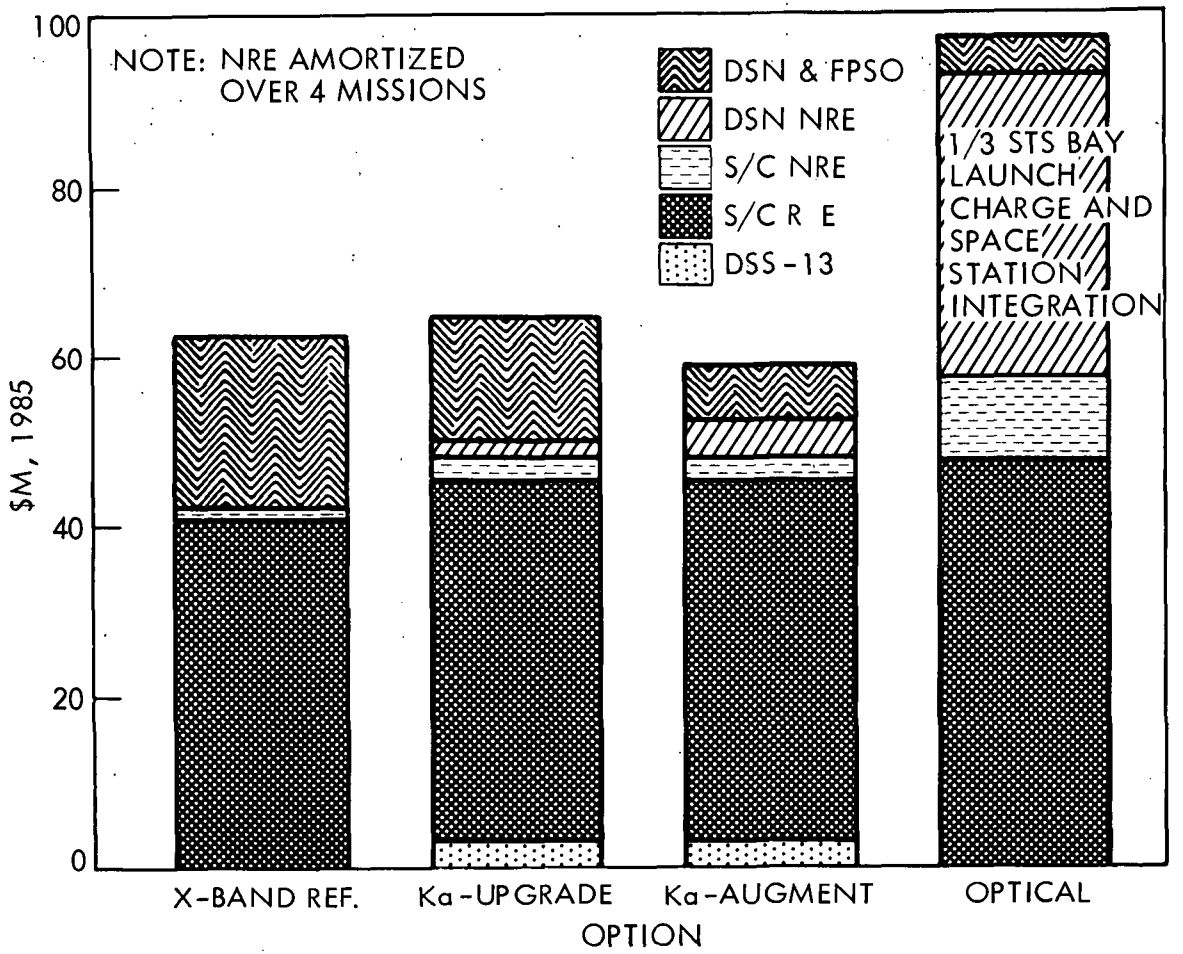

Figure 19. Outer Planet Data Return Option Costs

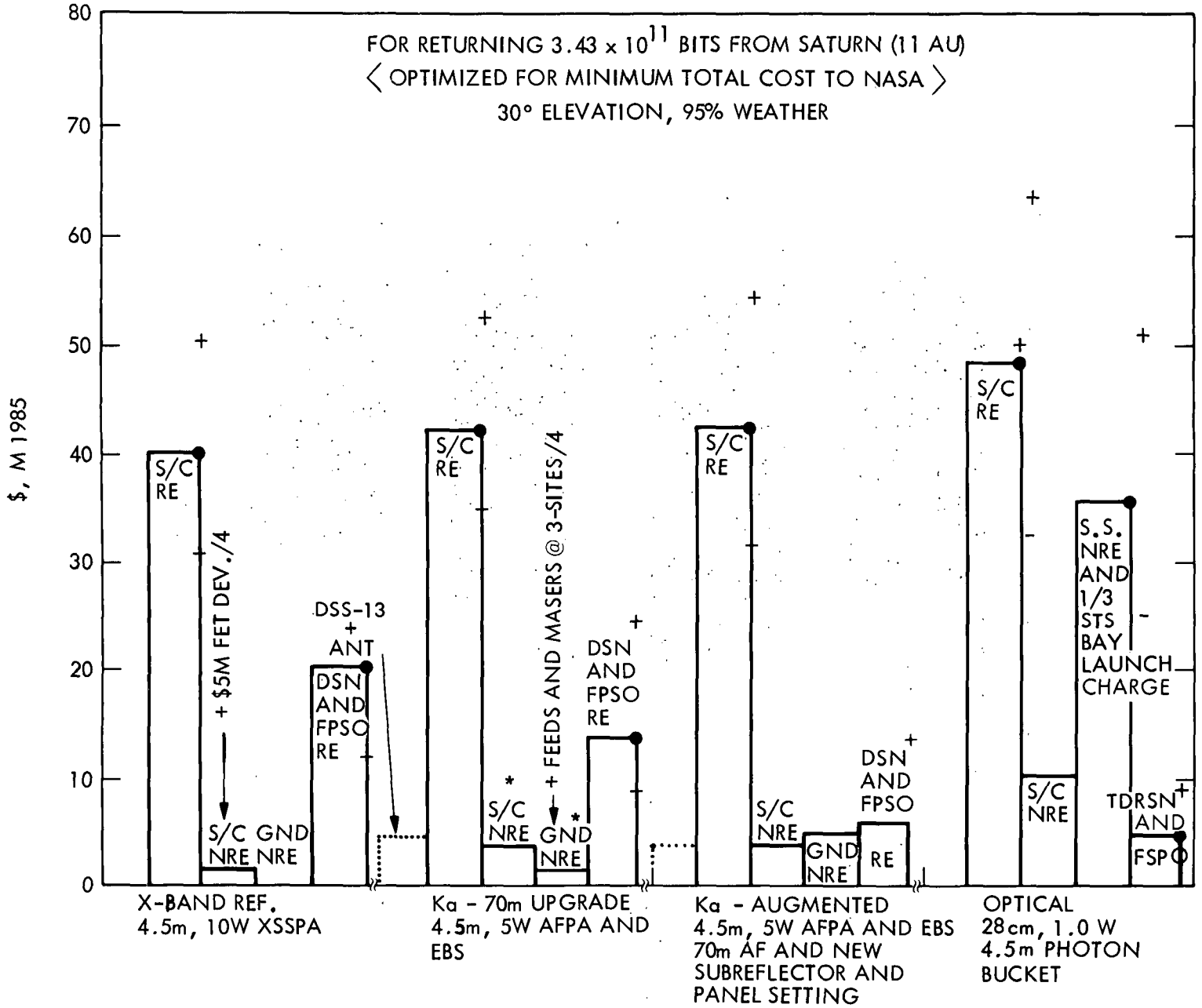

Figure 20. Outer Planet Data Return Option Cost Elements

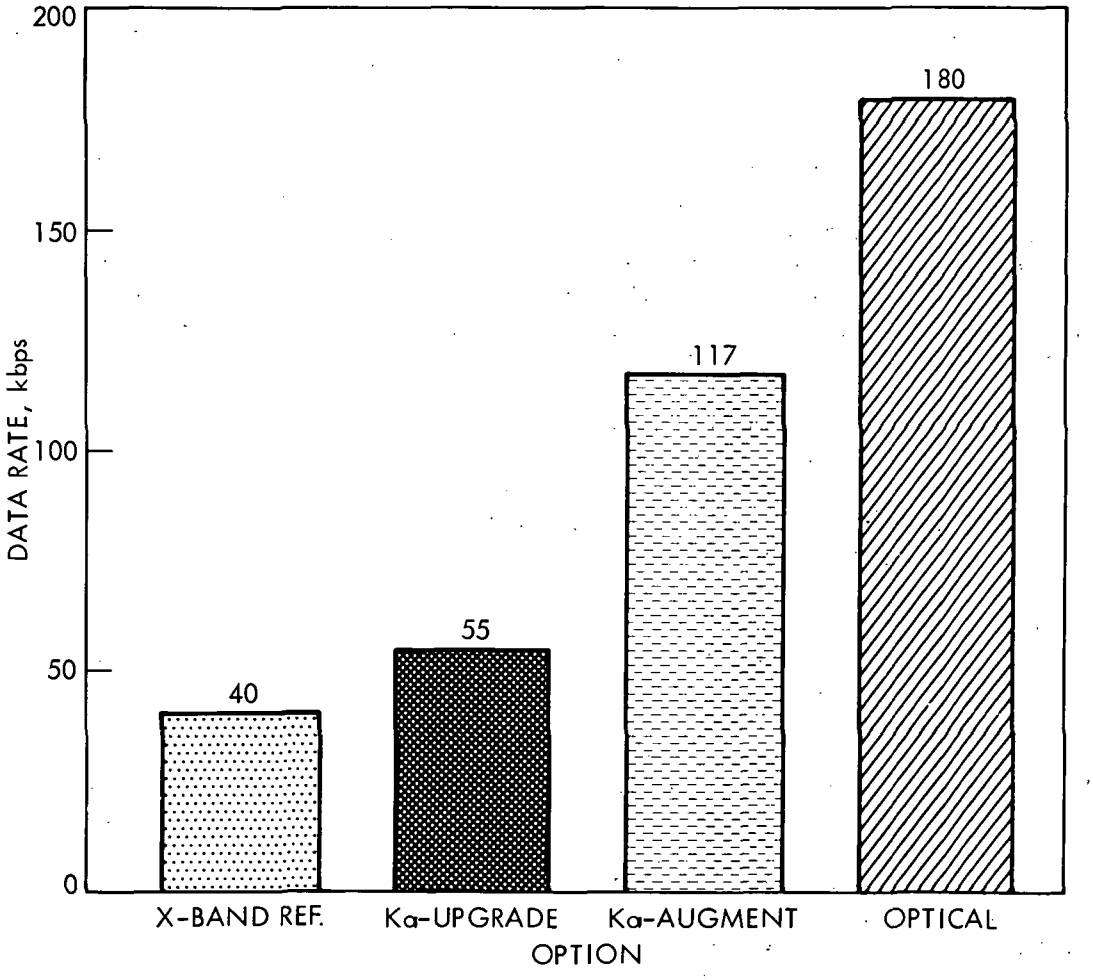

Figure 21. Outer Planet Data Return Optimum Rates

C. PERFORMANCE COMPARISON

Because of the shallow depth of study of the optical system, only the two microwave systems will be compared in technical performance. The performance comparison of an X-band, deep-space, telemetry return system and a Ka-band system is difficult because of the multitude of factors that must be considered. It is desirable to reduce the quantity of things to be compared to as few as possible in order to highlight the differences, but in so doing, some of the other considerations that should be weighed get short shrift, such as navigation and commanding and growth capability (and even emotional factors such as ever-fresh domains to explore in order to keep the staff on their toes). However, for this study the considerations will be limited in the simplified comparison to only the primary downlink telemetry return advantage or disadvantage factors.

The technical performance comparison shall be on the basis of spacecraft prime dc power input to achievable DSN data rate as output.

The context for setting the comparison will be given first. The engineering rationale for moving to higher frequencies is to take advantage of the fact that a given aperture diameter antenna will concentrate the electromagnetic radiation in a narrower angle, thus providing a higher incident flux density (W/m^2) on the receiver, all other things being equal. If all other things were equal (which they are not), the Ka-band system would have a $(32.0/8.415)^2$ or factor of 14.46 (11.602 dB) advantage over the X-band system.

This advantage could be employed to increase the spacecraft data rate by a factor of 14, or the spacecraft transmitter output radiated power (as distinct from prime dc power) could be decreased by $1/14^{th}$ or the spacecraft or ground antenna could be reduced in diameter by $\sqrt{14.46}$ (or a factor of 3.8, the RF frequency ratio or the beamwidth ratio).

The reader is cautioned that a single point description of the Ka- to X-band advantage is inadequate for describing a complex issue. By way of illustration, an example of a point comparison will be described for Canberra, but curves will also be shown to demonstrate the range of variation of one of the significant parameters, namely receiving-system noise temperatures. The "all other things" that are not equal are shown in Table 13, where the differences are shown in the aperture efficiencies of the DSN 70-m antennas at X- and Ka-band due to reflecting surface finish and position, RF circuit losses, atmospheric turbulence phase error effects, and other frequency sensitive factors. Even with the active compensation of distortion and other environment-induced phase errors, and better closed-loop tracking performance, the Ka-band antenna will suffer a 1.02-dB efficiency loss relative to the X-band antenna.

The next table entry compares the receiving-system noise temperatures at the two frequencies. The Canberra station is assumed for the comparison, as the weather effects are worse than Goldstone and the comparison is thus conservative, as an engineering safety factor in performance prediction. The comparison is done at a 30° elevation angle on the basis that 30° is

Table 13. Ka- and X-Band Performance Comparison

	X	Ka	Δ	Tol. dB
1. DSN 70m Antenna Efficiency	0.746	0.589%	-1.02 dB	±0.5
2. 70m Receiver Noise Temp.	21.766°K	51.041°K	-3.70 dB	+0.55 -0.44
3. Atmosphere Attenuation	0.574	0.076	-0.5 dB	+0.028 -0.088
4. Spacecraft Antenna Efficiency	0.4968	0.5475	+0.422 dB	+0.21 -0.28
5. Spacecraft dc-to-RF Conversion Efficiency	0.345	0.210	-2.16 dB	+0.56 -0.99
		Net Losses	-6.958 dB	+0.955 -1.229
		Theoretical Gain	+11.602 dB	
		Ka-band Performance Advantages =	+4.699 dB	+0.95 -1.22

representative of the average of the operational angles for tracking deep-space missions. At lower elevation angles the comparison will be much worse, and at higher elevation angles the comparison will not be as bad for Ka-band. Also in this performance comparison factor is the associated weather model, which was taken to be the 90% model.

Figures 22 and 23 show the ratio in dB of the X- and Ka-band receiving-system noise temperatures as a function of elevation angle and percent weather for Goldstone and Canberra or Madrid. From these curves, one can see the difficulty of stating a single Figure for the Ka- and X-band advantage.

Figure 24 (private communication from M. Koerner) shows the ratio in dB of Ka- to X-band achievable data rate for the same dc power input aboard the spacecraft. A 2.09-dB difference in dc-to-RF conversion efficiency is assumed along with a -1-dB pointing loss at either frequency. The system tolerances are convolved with the weather model to yield the curves of the ratio as a function of elevation angle with link reliability as a parameter and for the two classes of sites.

The next table entry is the difference in the atmosphere attenuation at the two frequencies. A difference of about 1/2 dB based on the Canberra 30° elevation, 90% weather conditions.

The spacecraft antenna aperture efficiency, including pointing losses, and transmission line differences, is shown in the next table entry. This comparison is favorable to Ka-band due to the array-feed power amplifier not having the transmission line losses inherent in the selected X-band design. (An array feed at X-band could also be developed to overcome the Cassegrain single-horn feed, transmission-line losses from the spacecraft bus-located RF power amplifier at increased cost, of course, but this comparison was done for the conventional, existing X-Cassegrain versus a Ka-band array-feed power amplifier.)

The last table entry compares the efficiency of the two different frequency RF power amplifiers in converting the spacecraft prime dc power into RF power. The higher frequency suffers due to: increased skin-effect, current conductor losses; the surface finish and mechanical fabrication tolerances; reproducible technique experience and foundary or oven yields; beam focus accuracy; beam or current interceptions; secondary electron production; uniformity of beam or wafer current distributions; junction effects; scalability to higher frequencies; modeling accuracies; limitations of power level scaling; larger ceramic dielectric losses at higher frequencies; solid-state device mobilities approaching relaxation times; closer-spaced semiconductor lines resulting in greater breakdown potential that necessitates a lower voltage and higher currents for a given power level, thus adding to the $I^2 R$ losses; etc.

The net advantage of Ka-band relative to X-band for the return of deep-space planetary exploration telemetry when compared on the basis of spacecraft input prime dc power to data rate achieved at the DSN's most adverse weather station (Canberra) is 4.64 dB, +0.95/-1.23, or a factor of 2.9 in data rate. The curves of Figure 24 illustrate that the advantage is higher at Goldstone and show the variation with elevation angle and link reliability. The

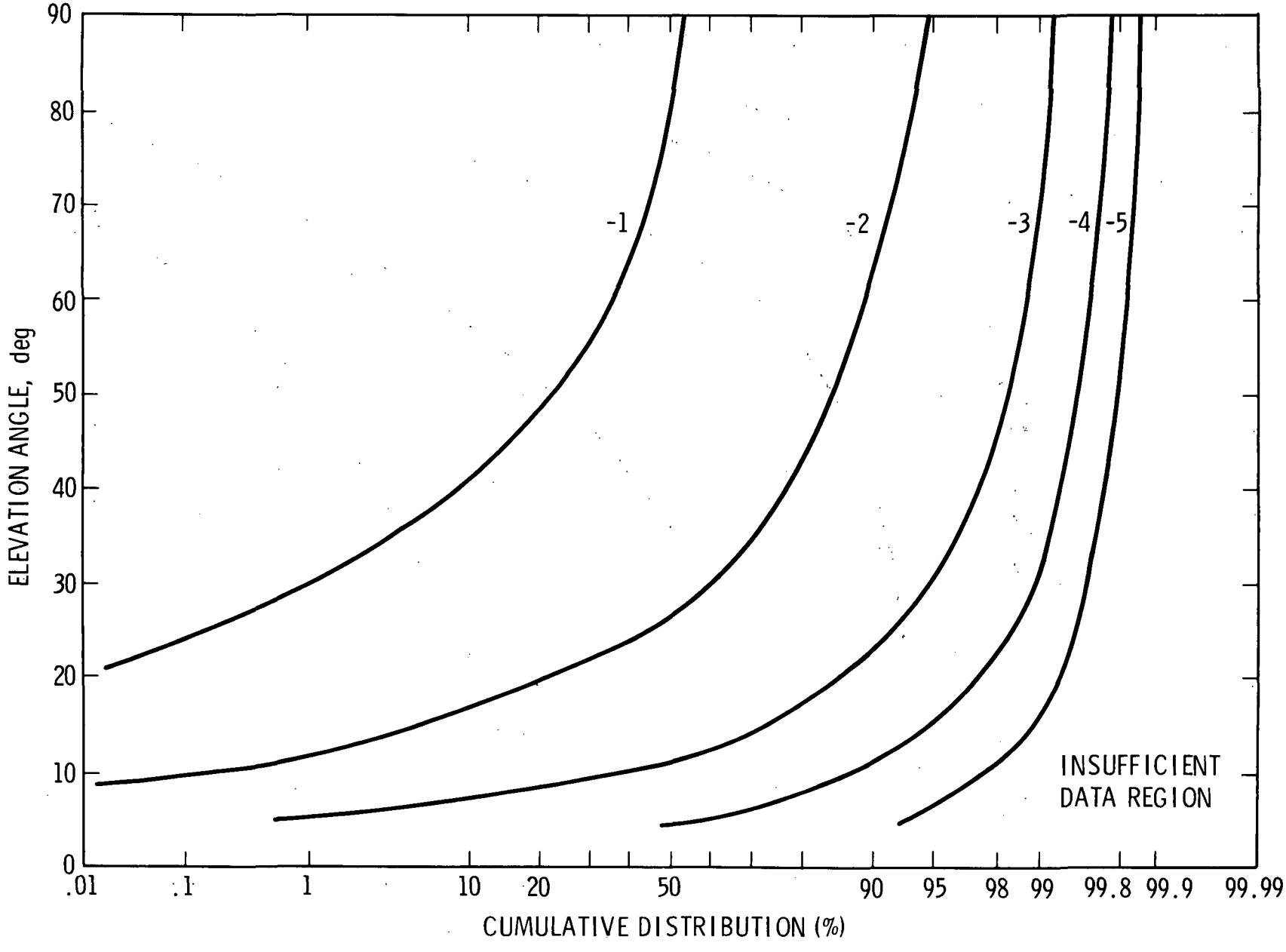

Figure 22. Goldstone X- and Ka-Band Receiving System Noise Temperature Ratio Contours

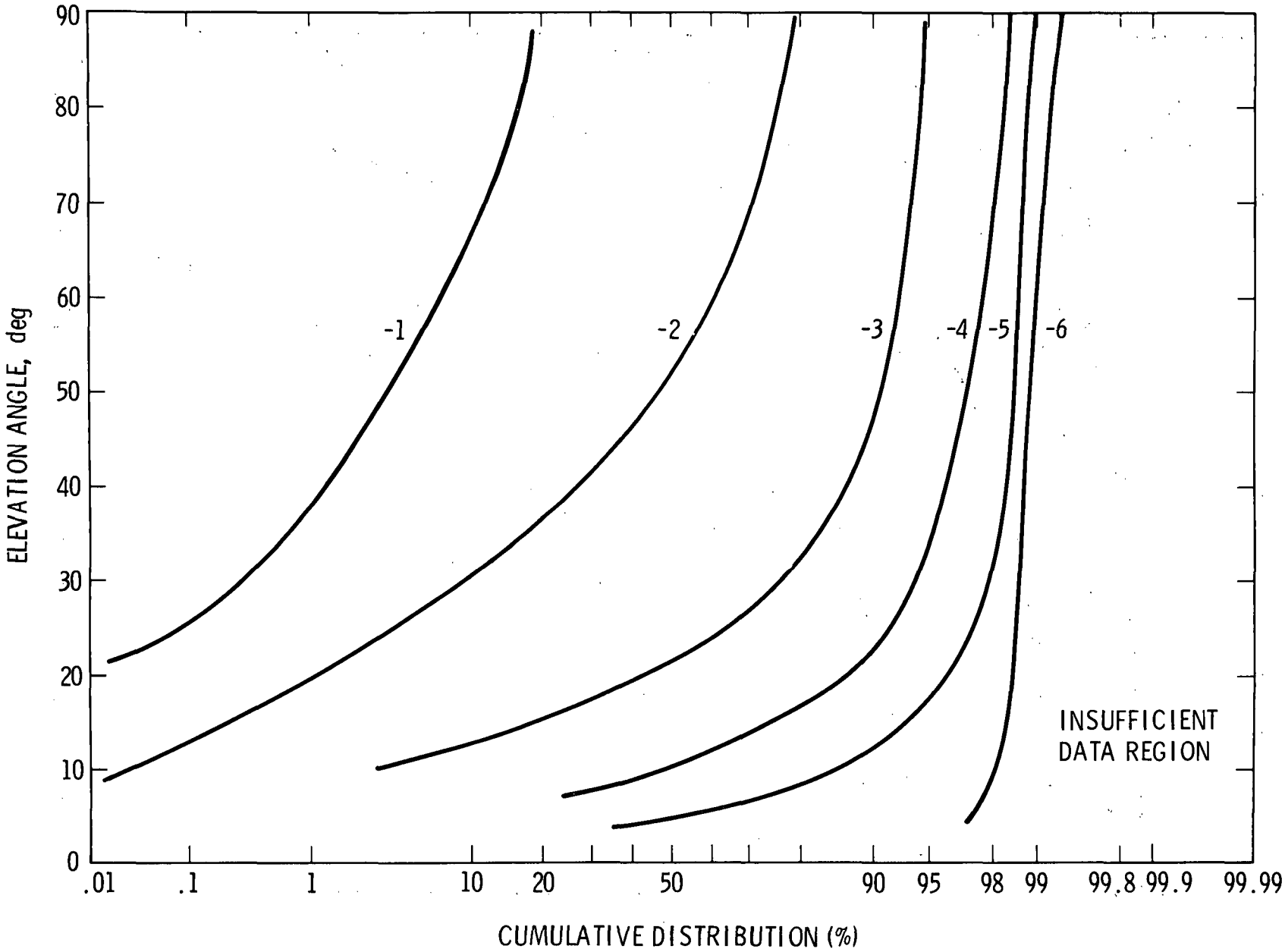

Figure 23. Madrid or Canberra X- and Ka-Band Receiving System Noise Temperature Ratio Contours

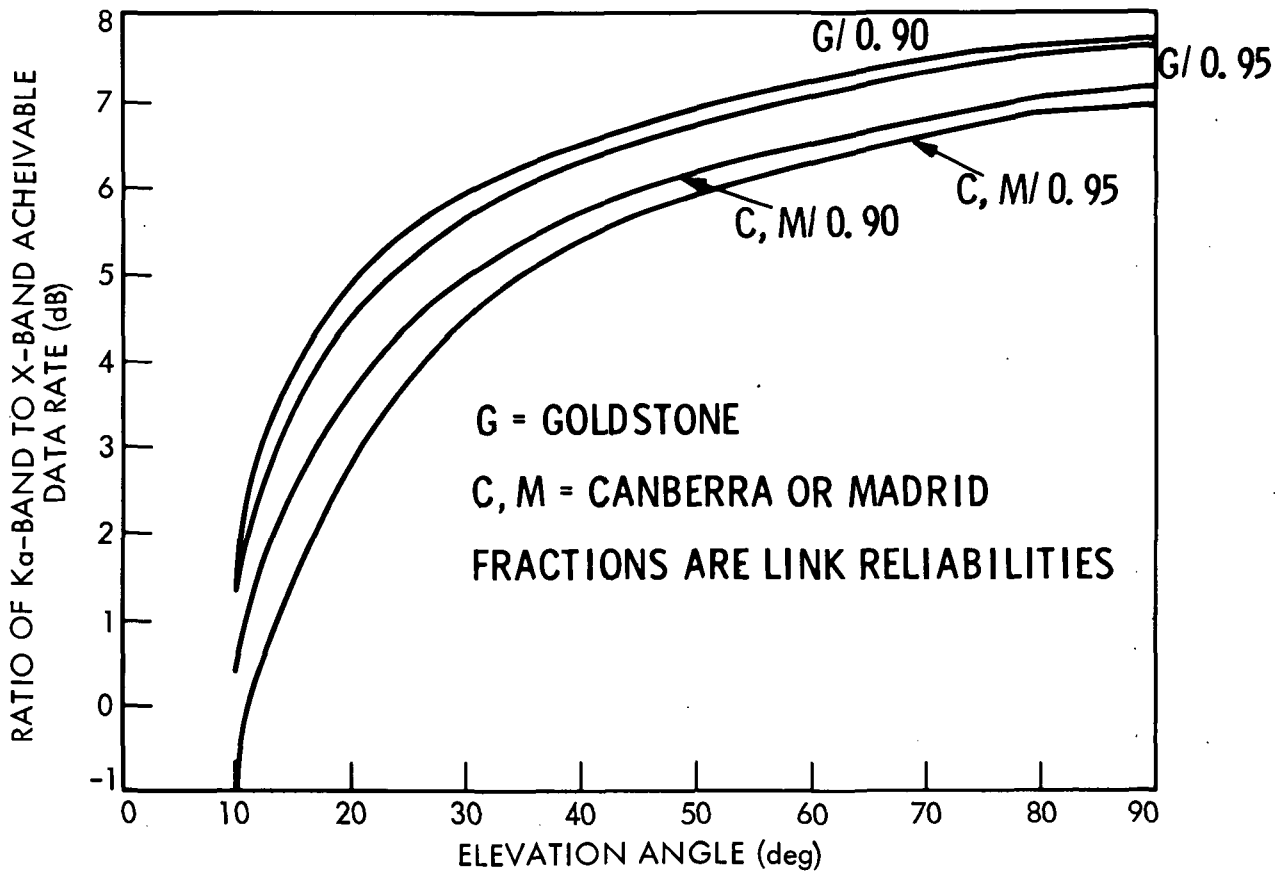

Figure 24. Ka-Band Telemetry Performance Advantage Over X-Band

relative advantage of Ka-band can be enhanced by operating in a burst mode at the higher elevation angles and over the more favorable site.

The burst-mode option study should address considerations of spacecraft data storage playback rate capability, energy storage and conversion device efficiency, mass, and costs, as well as the potential for increased dc-to-RF power conversion efficiency when operating at higher power output levels.

A composite figure representing the Ka- and X-band performance advantage of all the DSN sites with achievable data rates tailored to elevation angles would be an interesting figure to derive in the future.

SECTION V

CONCLUSIONS AND RECOMMENDATIONS

A. CONCLUSIONS

1. Ka-band has a definite performance advantage over X-band, depending upon the Earth receiving-site weather and the DSN antenna elevation angle (Figure 24). For a 0.90 reliability link at Goldstone, the advantage, in terms of the ratio of achievable data rates at the DSN for the same dc-power input to the spacecraft, is 6.8 dB (σ = 0.70 dB) at 50° elevation angle and 2.4 dB (σ = 0.67 dB) at 10° elevation. Corresponding dB ratios for Canberra/Madrid are 6.2 dB and 0.5 dB. For 0.95 link reliability, the dB ratios are 6.7 dB and 1.3 dB at Goldstone, and 5.9 dB and -0.8 dB at the other sites.

2. The difference in cost between X-band and Ka-band telecommunications systems is small and much less than the uncertainty in the cost estimate.

3. Antenna pointing at Ka-band will be achieved by use of more accurate sensors and positioning techniques aboard the spacecraft and on the ground. Compared to the existing X-band capabilities (0.005° DSN and 0.18° spacecraft), electronic beam steering of an array-feed power amplifier (phased array) aboard the spacecraft and a 7-element array-feed active combiner at the DSN antenna equipped with an optic gyro, will provide the required increase in pointing-angle accuracy (the ratio of the RF frequencies).

4. Compared to X-band, the dc-to-RF power conversion efficiency of spacecraft amplifiers at Ka-band with less than 10 W output power levels, is about -2 dB, with an uncertainty of +0.6 dB and -1 dB.

5. Improved weather models for specific DSN sites and improved weather effects models which currently yield over $\pm$10% system-noise temperature uncertainties, could permit a reduced performance margin requirement that could gain over a dB in link performance. Also, such data and techniques could assist in the design of the acquisition system for severe weather conditions at low elevation angles (where acquisition and handover will be difficult).

6. There are two technically viable candidates for providing the required compensations at Ka-band for environmentally induced distortions of the DSN 70-m antennas. Whether accomplished through electronic means with adaptive feed arrays, or with mechanical means employing panel positioners, both cost estimates are in the same ballpark, with the electronic-array approach estimating lower cost, but a larger uncertainty.

7. The cost to the spacecraft of providing the telemetry function is more than just the classical radio subsystem cost. Not only should the high-gain antenna structure be included, but also a portion of the attitude control and propulsion subsystems that are necessary for utilizing the narrow-beam antenna gain. The total cost is approximately double the radio subsystem cost.

8. Optical system costs are currently about 40% greater than microwave systems. The costs are more uncertain and larger because of less-mature technology and the requirement to both transport to orbit and to assemble a new infrastructure representing the DSN-terminal-in-the-sky.

B. DISCUSSION

1. To improve the accuracy and extend the range, the cost model needs to be refined by:

a) incorporating a process akin to the SRM technique of cost estimation so as to include all of the labor, service, and overhead charges and to include the review process by section and division managers for completeness and accuracy;

b) including a more detailed model of the ground portion or Earth-orbiting portions of the overall telemetry link;

c) including the effects of quantization of parameters such as RTG 25-W increments, fixed DSN-antenna sizes, data-rate multiples, maximum spacecraft solid-antenna size, leased data lines capacities and rates, etc.;

d) including second order variations of cost of mass transport and power with data storage quantities, pointing sensor and actuator accuracies, data compression ratios, etc.;

e) developing the methodology for trades among data compression, data storage and retrieval rates, and telemetry data rates and periods; and

f) including provisions for separately displaying costs by the various segments involved in the process, such as design, transportation, end-to-end data system, flight project office, TDA area, headquarters code, etc.

2. It is desirable to have cost data of more uniform pedigree and accuracy. Some data was collected from knowledgeable sources, not all of it reflects the same degree of uncertainty, and some data is the author's estimates.

3. The microwave systems costs are relatively comparable (both done bottom-up, most data inputs provided by the same persons); however, the optical system cost is not comparable (top-down, and so different from the

microwave systems that it is based off-Earth). Thus, X- and Ka-band comparisons of costs would be less uncertain than comparing X- or Ka-band with optics costs.

4. There is an advantage to NASA in the form of overall cost minimization if more capable spacecraft are flown, because the balance between spacecraft and ground costs are better. Thus, it is undesirable for the flight projects to simply cut back on spacecraft eirp in order to reduce the spacecraft cost, as that will result in the DSN having to devote more time and resources to tracking for longer time periods the data return from the mission. This may lead to not tracking other missions in flight, which is a waste of their data (representing a loss to NASA), or having to construct added apertures in order to track all users simultaneously, or having to pay rent to other agencies in order to acquire enough aperture to permit the spacecraft to increase its data rate in order to time share the receiving resource among all users.

5. This study has assumed that the spacecraft would transmit only at the very highest data rate whenever needed and would use the largest DSN antennas (or largest conceivable optical collector) in order to do so. The high data rate does encompass the majority of the data to be returned. This may be adequate for purposes of driving out X- and Ka-band differences, but it ignores slow data acquisition periods such as during cruise. By expanding the trade study parameters and increasing the model complexity, it would be more accurate in future to include the variable data-rate downlink telemetry periods in the overall costing.

C. RECOMMENDATIONS

1. Continue developing both Ka-band and optical frequency options for future deep-space communications to permit each mission to select the optimum frequency.

2. Continue to perform detailed trade studies of the telecom systems (including pointing subsystem requirements) for deep-space exploration missions, with consideration for constrained DSN tracking time and low-Earth-orbiting station view periods.

3. Develop high dc-to-RF power conversion efficiency and long life devices for power amplifying Ka-band signals and for optical wavelength lasers.

4. Examine techniques and develop methods for separately minimizing the telecom cost to flight projects, the cost of tracking time for the DSN, and the overall cost to NASA.

5. Develop techniques for performing trades between data compression and telecom link performance.

6. Develop techniques for determining the selection of:

   a) the optimum receiving aperture size to schedule for a mission or for a particular phase of a mission;

   b) the most cost-effective optical photon bucket diameters in orbit or on the ground; or

   c) the optimum DSN network: 70 m, 34 m, 34-m arrayed with 34 m, 34-m arrayed with 70 m, augmented 70-m arrays with other agencies, etc.

7. Get Ka-band and optical frequency beacons in deep space as soon as possible for the DSN to begin developing actual tracking weather statistics for developing engineering design confidence.

8. Develop the performance and cost models in detail for 70-m antenna array-feed and panel-positioning environment distortion-correcting techniques.

9. Develop models, analysis techniques, and experiments for the optical astrometric navigation data systems.

10. Begin a detailed investigation of the interfaces aboard the Space Station for a deep-space optical communication and tracking terminal.

11. Examine the technology status for a large photon bucket and uplink laser for space-based, deep-space optical tracking functions.

12. Examine the network interfaces and control aspects of a Space Station based, deep-space optical terminal.

13. Study, in more detail, the spacecraft configurations and interfaces for Ka-band and optical transponders and power amplifiers.

14. Conduct a detailed configuration and performance assessment of Ka-band, X-band, and optical links on the Mars Sample Return Mission telecom requirements.

15. Examine strategies for mitigating the effects of weather on Ka-band and Earth-based optical links, such as selective heavy coding for critical data [Ref. 12], store and dump operating modes for the spacecraft or burst-mode communications, site diversity, beamed waveguides, etc.

SECTION VI

LIST OF REFERENCES

1. Dickinson, R., "X-band vs. Ka-band Cost Trade Study Preliminary Results," Internal JPL Memo to D. Rea, Nov. 6, 1984.

2. Neugebauer, M.M., "Mariner Mark II and the Exploration of the Solar System," Science, Vol. 219, Feb. 4, 1983, pp. 443-449.

3. Draper, R.F., "The Mariner Mark II Program," AIAA-84-0214, AIAA 22nd Aerospace Sciences Meeting, Reno, Nevada, Jan. 9-12, 1984.

4. Potter, P., M. Shumate, C. Stelzreid, and W. Wells, "A Study of Weather-Dependent Data Links for Deep Space Applications," Jet Propulsion Laboratory Technical Report 32-1392 (internal document), Pasadena, CA, Oct. 15, 1969.

5. Rakiewicz, J., "OSSA MMKII CRAF Mission Operations System Requirements and Preliminary Design, 699-500," Jet Propulsion Laboratory JPL D-1391, Rev. B (internal document), Jan. 23, 1985.

6. de Vries, J.P., H.N. Norton, and D.P. Blanchard, "Mars Sample Return Mission, 1984 Study Report," Jet Propulsion Laboratory, JPL D-1845 (internal document), Pasadena, CA, Sept. 28, 1984.

7. Clauss, R., M. Franco, and S. Slobin, "Ka-Band Weather-Dependent System Performance Estimates for Goldstone," The Telecommunications and Data Acquisition Progress Report 42-71, Jet Propulsion Laboratory, July-Sept. 1982, pp. 60-65.

8. "Deep Space Network/Flight Project Interface Design Handbook," Jet Propulsion Laboratory JPL 810-5, Rev. D (internal document), Feb. 1984.

9. Kerr, D.E., "Propagation of Short Radio Waves," Radiation Laboratory Series, Vol. 13, McGraw-Hill, N.Y., 1951.

10. Potter, P., "64-Meter Antenna Operation at Ka-Band," The Telecommunications and Data Acquisition Progress Report 42-57, Jet Propulsion Laboratory, March-April 1980, p. 65-70.

11. "NASA Space Systems Technology Model, Vol. IIA," Space Technology Trends and Forecasts, Fifth Issue, NASA OAST Code RS, Washington, DC 20546, Jan. 1984, p. 12.

12. Swanson, L. and J. Yuen, "A Strategy for Successful Deep Space Information Transmission in Bad Weather," The Telecommunications and Data Acquisition Progress Report 42-78, Jet Propulsion Laboratory, April-June 1984, pp. 143-151.